

Tides, Interactions, and Fine-Scale Substructures in Galaxy Clusters

Christopher J. Conselice¹ and John S. Gallagher III

Department of Astronomy, University of Wisconsin, Madison, 475 N. Charter St., Madison, WI., 53706

ABSTRACT

We present the results of a study on galaxy interactions, tides, and other processes which produce luminous fine-scale substructures in the galaxy clusters: Coma, Perseus, Abell 2199, AWM 3 and AWM 5. All unusual structures in these clusters can be categorized in seven morphologies: interacting galaxies, multiple galaxies (non-interacting), distorted galaxies, tailed galaxies, line galaxies, dwarf galaxy groups and galaxy aggregates. The various morphologies are described, and a catalog is presented of 248 objects in these five clusters along with color, and positional information obtained from CCD images taken with the WIYN 3.5m telescope in broadband B and R filters.

Distorted, interacting, and fine-scale substructures have a range of colors extending from blue objects with $B-R \approx 0$, to redder colors at $B-R \approx 2.5$. We also find that the structures with the most disturbed morphology have the bluest colors. Additionally, the relative number distributions of these structures, suggests that two separate classes of galaxy clusters exist: one dominated by distorted structures and the other dominated by galaxy associations. The Coma and Perseus clusters, respectively, are proposed as models for these types of clusters. These structures avoid the deep potentials of the dominant D or cD galaxies in the Coma and Perseus clusters, and tend to clump together.

Possible mechanisms for the production of fine-scale substructure are reviewed and compared to observations of $z \approx 0.4$ Butcher-Oemler clusters. We conclude, based on color, positional, and statistical data, that the most likely mechanism for the creation of these structures is through an interaction with the gravitational potential of the cluster, possibly coupled with effects of weak interactions with large cluster ellipticals.

Subject headings: galaxies - clusters - individual (Coma Abell 1656, Perseus, Abell 2199, AWM 3, AWM5) : galaxies - formation : galaxies- interactions : galaxies - evolution.

¹chris@astro.wisc.edu

1. INTRODUCTION

Galaxy interactions and mergers have been recognized since the work of Toomre and Toomre (1972) as an important, if not the crucial aspect, for understanding galaxy evolution (see Schweizer, 1986 and Barnes & Hernquist, 1992 for reviews). Since very few galaxies are isolated (Ramella et al. 1989 and references therein), galaxy evolution must occur for the majority of galaxies in a dense cluster, or group environment, facilitating interactions. Also, galaxy clusters in general are not relaxed systems (e.g. West 1994; Girardi et al. 1997), and by definition have an enhanced number density of galaxies. If clusters are not virialized, an increased number of interactions likely will occur among member galaxies. Furthermore, clusters are probably in part created hierarchically through accretion of field galaxies, possibly accounting for the large proportion of blue galaxies in rich clusters at high redshifts (Butcher & Oemler 1978, hereafter B-O effect); this process, or one similar to it, might be occurring in nearby clusters at a reduced rate, with similar observational consequences. The interplay between galaxy cluster formation and evolution, substructures in clusters and the morphological appearance of distant clusters can be further illuminated by studying the nature of interactions, tides and fine-scale substructures in nearby clusters. This paper is a morphological and physical study aimed at detecting and explaining these structures in the five nearby galaxy clusters: Coma, Perseus, Abell 2199, AWM 3 and AWM 5.

Distorted blue galaxies play a significant role in the evolution of clusters seen at moderate redshifts $z \approx 0.4$, first noticed in the work of Butcher and Oemler (1978, 1984). Using the high resolution capabilities of the Hubble Space Telescopes, a high fraction of the blue galaxies in distant clusters were discovered to be either spirals, or distorted galaxies (Oemler, Dressler and Butcher 1997; Dressler et al. 1994; Couch et al. 1994). The origin of these objects is still a bit of a mystery. Many possible scenarios for the creation of B-O galaxies in distant clusters have been proposed: low-velocity galaxy-galaxy interactions (Icke 1985; Lavery & Henry 1988), interactions with a cluster gravitational potential (Henriksen and Byrd 1996; Valluri 1993; Byrd and Valtonen 1990), ram-pressure stripping (Gunn and Gott 1972; Dressler and Gunn 1983), and galaxy harassment (Moore, Lake and Katz, 1998). Many of these models are based on a scenario where a field galaxy falls into the cluster. If clusters are formed this way, hierarchically, then we should still see in-fall occurring, although at a much reduced rate (Kauffmann 1995). If we could locate which galaxies are in-falling into nearby clusters, this would give an excellent opportunity to test models which predict how clusters evolve, and determine which mechanisms are responsible for modifying field galaxies within clusters to yield the distinct galaxy populations in clusters (e.g. Dressler et al. 1997).

Another, and possibly related process involving interactions of galaxies in clusters, is the merger hypothesis for the creation of elliptical galaxies (e.g. Lake & Dressler 1986; Toomre 1977). The merger of galaxies has long been a popular explanation for the build up of the large central cD or D galaxies found at the centers of clusters (Ostriker and Tremaine 1975; Toomre 1978). In this model of galactic "cannibalism", a large central galaxy accretes nearby smaller galaxies, building

up its mass to become the giant galaxies we observe at the centers of rich clusters. Previous observations of cluster centers (Hoessel 1980; Schneider et al. 1983) have shown multiple nuclei to be common, present in at least 1/3 to 1/2 of all clusters. Projection effects are barely adequate to explain this high fraction of multiple nuclei observed in the cores of first ranked cD galaxies in clusters, and thus some are possibly remnants of cannibalized galaxies. There are however, some objections to modelling the formation of the more common cluster ellipticals as being solely a result of mergers (e.g. Gunn 1987; van den Bergh 1982).

A less studied feature of nearby cluster evolution is the possibility of interactions, mergers and stripping occurring in nearby galaxy clusters. Early work on this topic included indirect studies on the sizes of cluster galaxies, suggesting that the sizes of the ellipticals shrink as they get closer to the core of the cluster (Strom & Strom, 1978). This shrinkage was attributed to stripping of material from the galaxies closest to the center. Some later studies have however disputed this result (Currie 1983), interpreting the Strom and Strom trend as an effect of luminosity segregation in clusters. Another form of distorted galaxy is the radio head-tail galaxies, well known features of clusters seen at radio wavelengths. Radio head-tail galaxies have been observed in several nearby clusters, including Coma and Perseus (e.g. Owen and Eilek 1998). The usual interpretation given for the existence of these tails is a scenario where an in-falling galaxy is losing gas from an interaction with the intracluster medium; however, internal dynamical causes cannot be completely excluded.

Additionally, there are several possible interacting galaxies and merger remnants in nearby clusters. Less rich clusters such as Virgo and Fornax, contain possible low-velocity galaxy-galaxy interactions, as well as distorted galaxies. One example, NGC 4438/35 in the Virgo cluster, is a pair of galaxies displaying a distorted morphology in both optical and radio (CO and HI) emission (Kenney et al. 1995). Another Virgo galaxy, the Sa NGC 4424 is probably the result of a merger (Kenney et al. 1996). A quantitative study of 84 Virgo disk galaxies (Koopmann and Kenney 1998) shows a systematic bias in previous morphological studies towards early Hubble type classification, yet the physical properties of these galaxies other than their morphological Hubble types, suggest they are physically related to later type galaxies. This change in morphology is possibly the result of stripping and galaxy interactions changing slightly the morphology of the galaxies in Virgo. Rich clusters, which are generally thought of as being more dynamically stable and mature systems, do not have as many examples of luminous interacting systems. However, NGC 4676, “the Mice” is one of the best examples of a low-velocity galaxy-galaxy interaction and is on the Coma cluster’s outskirts. This galaxy pair is the result of a two disk galaxy merger (Barnes 1998). Despite these dynamical and observational examples of interacting and distorted galaxies in clusters, there has been no attempt to systematically classify and study these systems in nearby clusters.

This paper presents results from a morphological study of fields in nearby galaxy clusters based on moderately deep B and R images of clusters taken with the WIYN 3.5m telescope. We use these images to systematically investigate the types, distributions, frequency of, and physical

features which could be associated with interactions, tides or stripping in clusters. Because such processes tend to produce anomalous light distributions on galactic, or smaller scales, we refer to such features by the generic term 'fine-scale substructures'. Since this is a morphological survey, follow-up measurements are required to prove that any particular fine scale substructure is in a given cluster. We carried out our survey looking for galaxies which have morphological properties of galaxy interactions, or distortions, and to investigate any fine-scale substructures in the clusters: Abell 2199, Coma, Perseus, AWM 3 and AWM 5. We show that all structures found in these clusters of various richness and morphology can be classified into just seven different categories: Multiple Galaxies (MG), Galaxy Interactions (IG), dwarf galaxies groups (dwG), tailed galaxies (TG), and distorted galaxies (DG), line galaxies (LG), and galaxy aggregates (AG). In this paper we describe these different morphologies, present color, magnitude, and positional information, and discuss possible origins for the existence of these structures, including comparisons to models.

Processes similar to those responsible for creating the large fractions of distorted galaxies at moderate redshifts are probably occurring in nearby clusters, albeit at lower levels. We further propose that the mechanism producing most of these disturbed galaxies is via a method similar to the proposed galaxy harassment models (Moore et al. 1998). The drop-off in severity of distorted morphologies in clusters from $z \approx 0.4$ to $z \approx 0$ can be accounted for by the decayed rate of in-falling galaxies in hierarchical clustering, which is theoretically predicted to peak at moderate redshifts (Kauffmann 1995), or from the longer dynamical time scales associated with disturbing lower-mass (and hence lower luminous) galaxies.

2. OBSERVATIONS AND METHOD

All of the observations used in this paper were obtained with the WIYN² 3.5m, f/6.2 telescope located at Kitt Peak National Observatory. A thinned 2048² pixel S2kB charged coupled device (CCD) was used to image the cluster fields, mostly in or near cluster cores. The resulting images are at a scale of 0.2 arcsec per pixel, and cover a field-of-view of 6.8 x 6.8 arcmin. The Coma, Abell 2199, AWM 3 and AWM 5 clusters were imaged between the nights of May 31 to June 2 1997. The Coma cluster core was imaged in 6 different fields (see Table 1), straddled by the two D galaxies NGC 4874 and NGC 4889. Two additional fields in Coma were taken centered on NGC 4881 and IC 4051. One field image for Abell 2199, AWM 3 and AWM5, centered about their cD galaxies were also taken. Exposure times were 900s for the B-band and 600s for the R-band. The seeing ranged from 0.7 to 1 arcseconds full width at half maximum. The Perseus cluster was imaged in the fall on 1996, when the WIYN CCD was non-linear. We do not present photometric information for this cluster due to the uncertainty in the performance of the CCD.

²The WIYN Observatory is a joint facility of the University of Wisconsin-Madison, Indiana University, Yale University, and the National Optical Astronomy Observatories.

The non-linearity does not affect the high-resolution image quality of the cluster, and we are still able to make positive morphological identifications of galaxies in the cluster. We also obtained, as a control sample for identification of background galaxies, a field centered on the Hubble Deep Field (Williams et al. 1996). We chose this area for its known lack of nearby clusters, galaxies and stars, as well as for its low Galactic extinction.

All of the images were then searched by eye, examining in detail, every region of each image in the R and B bands. Interesting features, distorted galaxies, multiple galaxies, or anything unusual was noted. For the images centered on NGC 4881, IC 4051, AWM 5 and AWM 3, there exists a large central galaxy. These galaxies were removed using the IRAF routines “isophote” and “bmodel” for the less crowded fields. Subtracting the central galaxy yields a better view of the entire cluster, particularly the central part of the core. In the denser fields, where bmodel and isophote produce significant artifacts due to the presence of field galaxies, the central galaxies were removed using a 180° rotation about their centers and subtracted out in a manner similar to that presented by Conselice (1997). The symmetry method allows a clearer view of the cores of these large E galaxies, nearly all of which show some form of distortion, or have multiple nuclei.

Initially, the images were searched for unusual or outstanding features, without reference to any distorted galaxy morphological system. Each object’s position and a description of it were recorded. By a closer examination of the list of structures, we created a catalog of all the unusual objects in our cluster fields, and found that all structures (248 total) could be classified into seven different categories.

We then performed aperture photometry on the core of each structure, to determine both colors and magnitudes; only the core of each structure was measured to maximize our S/N ratio, and to provide a guide for future spectroscopic studies. We use Landolt (1992) standard stars to calibrate our images and are able to obtain photometry with errors typically less than 0.1 magnitudes. We do not attempt to obtain color and magnitude information for entire galaxies. The tidal and distorted features are typically faint and photometry of these features is not possible with our relatively shallow imaging; deeper images are necessary before we can obtain photometry of these fainter features. In our comparison blank field, we performed the same kind of analysis, looking for any unusual structures that are ubiquitous to a random area of the sky. From this comparison field, we are able to put constraints on the background contamination in our cluster images.

3. SAMPLE

Our sample includes the Coma (Abell 1656), Perseus (Abell 0426), AWM 3, AWM 5, and Abell 2199 clusters. What follows is a brief summary of what is known about these clusters and their relationship to any possible structures.

3.1. Coma Cluster

The Coma Cluster with a radial velocity of 6942 km s^{-1} ($z \approx 0.023$), is the prototypical rich cluster and the most exhaustively studied rich cluster in history³, with a BM (Bautz and Morgan 1970) richness class of II (see Biviano 1997 for a recent review).

Coma at large scales has a compact symmetrical spherical shape (Kent and Gunn, 1982), and until the X-ray work of Johnson et al. (1978) was generally assumed to be a relaxed, virialized cluster. The amount and intensity of X-ray inhomogeneity and substructure recognized in Coma has increased over the past few years, particularly with ROSAT (Briel, Henry and Bohringer 1992; White Briel and Henry 1993). Additionally, the observed X-ray emission cannot be completely modeled by an isothermal distribution (Henriksen 1985).

X-ray substructure is the most obvious form, but substructure also exists at optical wavelengths. The best example of substructure in Coma is the existence of two D galaxies, NGC 4874 and NGC 4889, both with similar masses. D galaxies are the central locations of deep potential wells (Beers and Geller 1983), and the existence of two in Coma suggests that the cluster is not in complete virialized equilibrium. Two-dimension image maps, analyzed by statistical maximum likelihood methods, also imply that the core of Coma is not in an equilibrium distribution (Fitchett and Webster 1987). Inspired by the amount of substructure seen in ROSAT maps, Colless and Dunn (1996) analyzed 552 Coma galaxy redshifts, finding that the velocity distributions can be fit by two Gaussians centered about the D galaxies NGC 4874 and NGC 4889, an effect first hinted at by Fitchett and Webster (1987). The general interpretation of this result is that the present Coma cluster formed sometime in the past by a merger between two clusters once centered about NGC 4874 and NGC 4889.

A less studied effect in Coma, as opposed to Virgo, is the presence of fine scale structures in its member galaxies. Searches for this type of feature is necessarily limited by the technology of telescopes and imaging techniques. In the last year or so, after the advent of new image processing and telescopes of high resolution capabilities, several fine scale structures have been found in Coma. Luminous arcs of material have been seen in several different areas of Coma (Trentham & Mobasher 1998; Secker 1998; this paper), and small dense 'galaxy aggregates' have been found (Conselice and Gallagher 1998). These arcs and aggregates are evidence for some form of interaction between galaxies, or between galaxies and the cluster potential. The bulk of this paper refers to fine scale substructures in Coma (116 in all), a significant portion of which are probably the result of physical effects similar to those which produced these arcs and aggregates.

³It may be argued that Coma is overtaking the less dense Virgo for the number one spot as the most intensively studied cluster. A search of the astro-ph preprint server shows that as of February 1998, there are 35 Coma papers, 27 Virgo and 19 on the Perseus cluster entered in the last year. This may be biased by a number of papers coming from the Coma meeting in Marseille in June, 1997, but still shows its growing popularity.

3.2. Perseus Cluster

The Perseus cluster (Abell 0426) is a relatively nearby cluster, $D \approx 75$ Mpc ($H_0 = 75$ km s $^{-1}$ Mpc $^{-1}$), with a moderate Galactic extinction, having a radial velocity of 5486 km s $^{-1}$ (z=0.0183) and BM class II-III. Compared to Coma, little attention has been given to Perseus in the past few decades.

Perseus contains a peculiar cD galaxy, NGC 1275 (Perseus A), which is a strong radio source. NGC 1275 is extremely distorted with filaments and abundant structure, and potentially has an origin that differs from other cD galaxies. Perseus differs from Coma in a few important areas. Perseus has only one large central galaxy, NGC 1275, as opposed to the two found in the Coma cluster. Perseus also has a compact core $R_c \approx 0.1$ Mpc and a high velocity dispersion $\sigma \approx 1260$ km s $^{-1}$, possibly related to the disturbed morphology of NGC 1275. Perseus also has a unimodal structure, with no significant optical substructure, as well as a regular velocity distribution (Girardi et al. 1997). However, both Slezak et al. (1994) and Mohr, Fabricant and Geller (1993) have found evidence for substructure in X-rays in this cluster. These X-ray studies are however limited to the central part of the cluster, and may be displaying effects of the central distorted galaxy NGC 1275, and the high velocity dispersion near the cluster center. Agreement between the ratio of the intracluster medium temperature and the velocity dispersion (β) for the entire cluster agrees well with theoretical predicted values. Therefore, for the most part, this cluster can be considered as virialized, with a possible recent significant in-fall event.

The Perseus cluster is also known to contain at least five examples of radio head-tail galaxies (Sijbring & DeBruyn 1998), including NGC 1275. These radio head-tail galaxies are generally interpreted as the result of an interaction between an in-falling galaxy and the intracluster medium (Sijbring & DeBruyn 1998). Head-tail galaxies, which these objects are usually referred to as, are only found in cluster. Perseus contains more of these objects than any other cluster (Sijbring & DeBruyn 1998). These radio tailed sources may also have a similar origin to the optical tailed galaxies as found in this study. In addition to having radio head-tail galaxies, Perseus contains a significant dwarf galaxy population, with the majority of these fragile systems showing neither evidence for an interaction, nor distorted morphologies (Gallagher Han and Wyse 1997).

3.3. Abell 2199

Abell 2199, is the richest cluster in our sample, with a BM richness class of I, and a radial velocity of 9063 km s $^{-1}$ (z≈0.032; $D \approx 120$ Mpc). This cluster is dominated by the cD cooling flow galaxy, NGC 6166. NGC 6166 has been the object of several detailed studies, and is the one of the best candidates for cD galaxy cannibalism (Pritchett & Harris 1990; Lauer 1986; Bridges et al. 1996; Conselice & Gallagher, 1998b). The core of NGC 6166 contains several distinct nuclei.

These objects are thought to be the remnants of merging elliptical galaxies which formed the cD, or are projection effects caused by eccentric orbits of isolated E galaxies (Lauer 1986).

Initial X-ray studies of Abell 2199 displayed a smooth distribution of emission with no evidence for substructure (Forman & Jones 1982). More recent X-ray images of this cluster reveal an elongated shape, as well as a significant cooling flow (Siddiqui, Stewart, and Johnstone 1998). Wang & Ulmer (1997) have found a strong correlation between X-ray elongation and the blue galaxy fraction. Abell 2199 has a flattened central distribution in both X-rays and optical light, and hence should have a high fraction of blue galaxies. Velocity dispersion work on this cluster has also shown that there exists a large number of galaxies that have negative peculiar velocities (Lucy et al. 1991). A recent study combining both X-ray and radio observations (Owen & Eilek 1998) indicates that the core of Abell 2199 is complex and cannot be described by a simple spherical cooling flow model. Maps of the overall velocity structure of Abell 2199 (Zabludoff, Huchra & Geller 1990), however, find no significant subclumps, or velocity structures, indicating that the core of Abell 2199 is virialized.

3.4. AWM 3 & AWM 5

These two clusters are among the set of poor clusters first studied by Morgan, Kayser & White (1975) and Albert, White & Morgan (1977). These Morgan poor clusters were initially identified from Palomar Sky-Survey prints as systems that contained large central D or cD galaxies, but lack the high number of normal luminosity members as seen in rich Abell clusters. A typical criterion for a AWM or MKW poor cluster is a system with 10 to 50 galaxies with magnitudes fainter than m_3+2 , where m_3 is the third ranked member of the cluster. AWM 5 is the furthest cluster in our sample with a radial velocity of 10346 km s^{-1} ($z \approx 0.035$), $D \approx 140 \text{ Mpc}$, and is centered about the cD galaxy NGC 6269. AWM 3 is the closest cluster in our sample with a radially velocity of 4497 km s^{-1} ($z \approx 0.015$) and a distance of $D \approx 60 \text{ Mpc}$.

These morphologically defined clusters were later shown to be physical systems with properties comparable to Abell clusters (Bahcall 1980). Additional X-ray studies (Kriss et al. 1983) revealed extended X-ray emission in these clusters. Galaxies in poor clusters also contain neutral hydrogen (Williams & Lynch 1991), as well as evidence for $\text{H}\alpha$ emission (Beers et al. 1984). These systems are also comparable in age to richer clusters, and contain a hot intracluster medium similar to those found in rich clusters (Price et al. 1991). In general, these Morgan poor clusters in both their X-ray and optical properties represent a class of objects that form a continuation from the rich Abell clusters towards galaxy groups; some having core densities comparable to those found in richer Abell clusters as well as similar X-ray properties (Bahcall 1980; Beers et al. 1984; Price et al. 1991).

4. THE CATALOGS

We found 248 examples of fine-scale substructures in the images of our five clusters. We can place every galaxy in our catalog into two broad categories: galaxy associations, and disturbed galaxies, with a third overlapping category, interacting galaxies, which are an association with a disturbed morphology. We can further divide these two broad categories into the seven distinct and more descriptive morphologies of line galaxies, distorted galaxies, multiple galaxies, tailed galaxies, interacting galaxies and galaxy aggregates (see Fig 1). The structures in our catalog are each assigned one of these morphological types. This initial approach is based purely on morphologies. As discussed in Section 5, some categories are likely to be dominated by contamination from background galaxies; not all fine scale structures seen towards a cluster are part of it.

Tables 6 through 10 contain our catalog of the fine-scale substructures found in our five clusters: Coma, Perseus, Abell 2199, AWM 3 and AWM 5. Column one contains the name of the object, starting with S (for structure) followed by the name of the cluster, and ending in a number. For the Coma cluster, we find a total of 116 structure, in Perseus 69, Abell 2199 30, AWM 5 with 23 and AWM 3 with 10 structures. Column two and three list the R.A. (J2000) and Dec. (J2000) for each structures. For Coma, Abell 2199, and AWM 5, columns four and five contain the R mag. and (B-R) color for each structures (see Section 2 for further explanation). The last two columns of Tables 6-10 list the morphological type, sometimes given with a ‘?’ to indicate that the identification is in doubt. Sometimes, the morphology changes between the R and B band images, and is noted in the last column.

The distance range between the closest and most distant galaxy in our sample is different by a factor of two, and it is possible that in the more distant clusters, we could be mistaking some morphological types for others. This is due to the degraded resolution seen in the more distant clusters. This is discussed in more detail in section 4.5. Briefly, this is a long standing problem for any morphological study, and can insert biases if not address appropriately. For this study, our resolution will only be degraded by a factor of two, and in other morphological studies concerning distant galaxies this is generally not enough to cause a change in morphology (Conselice et al. 1999, in prep). Additionally, physical features such as size, and (B-R) color are similar for each form of fine-scale substructure in each of our clusters, indicating that we are not overly biased by resolution degrading.

The following sections describe the different morphologies listed in the catalogs, giving possible field counterparts, and potential origins for each type of structure. We emphasize that our data are classifications of apparent galaxy structures, following the general approach used in previous galaxy catalogs (e.g. Arp 1966, Lauberts 1982, Arp & Madore 1987). Physical interpretations in many cases will require additional observations (see Sections 5 and 6). Comparisons to various models for the existence of these fine-scale substructures will be discussed in Section 7.

4.1. Distorted Galaxies

Distorted galaxies (DG), or peculiar galaxies have been observed in the field for decades (e.g. Arp 1966); as well as in distant clusters (e.g. Lavery & Henry 1998, 1994). The origin of these galaxies in the field is almost always attributed to some form of low-velocity galaxy-galaxy interaction. Distorted galaxies in the field are usually given the catch-all 'peculiar' classification. When a peculiar galaxy is isolated, it is either the result of a merger, or is a starburst galaxy, which can also be the result of a galaxy merger. The presence of distorted galaxies in nearby clusters is sometimes anecdotally noted, but has not been the subject of a focused morphological study. Nearly all of the disturbed morphologies in our sample could be classified in general terms as distorted normal galaxies, e.g. as expected from interactions. However, for the present purposes, distorted galaxies are a catch-all category that includes any isolated galaxy that has a peculiar structure and does not fit into the other categories. Galaxies that have a disturbed morphology, and have a nearby apparent companion, are classified as interacting galaxies, but may have a similar origin to distorted galaxies. For the purposes of this paper, we will classify large ellipticals, including cD galaxies, that have multiple nuclei (NGC 6166), or shells (NGC 5629) as distorted galaxies, with the understanding that not all distorted galaxies are caused by the same processes.

What could cause an apparently isolated galaxy in a cluster to be distorted? It is possible, although not likely, that an apparently single object is in reality an interacting pair, or a recent merger. In our sample we have about twice as many distorted galaxies as candidate interacting galaxies, and it would be hard to explain the existence of so many distorted galaxies by recent mergers. Many distorted galaxies could be products of past interactions, a model consistent with fast collisions in clusters where after effects linger (e.g. Moore et al. 1998). Alternatively, distorted galaxies could be interacting with the intracluster medium, producing a starburst, or with the cluster potential (see Section 7). The tidal radii (Merritt, 1984) for some of our distorted galaxies are consistent with stripping due to the cluster's potential, but some galaxies have stripped material which extends well beyond their gravitational tidal radii. Also, we see galaxies that are disturbed but are smaller than their tidal radius. However, by combining high-velocity galaxy interactions with tidal forces from the cluster potential, as predicted in galaxy harassment models (Moore et al. 1998), we may be able to explain distorted cluster galaxies. These models will be further discussed in Section 7.

4.2. Galaxy Aggregates

In a previous paper we have described the morphology of galaxy aggregates observed in the Coma cluster (Conselice & Gallagher, 1998a). A detailed description of these objects as seen in Coma is presented in that paper.

Aggregates are systems of galaxies inside clusters which are dominated by a central disk galaxy with smaller dwarf galaxies, or star knots surrounding it in an asymmetrical pattern; generally all on one side. The colors of the smaller members tends to vary according to the specific aggregate. Some of the Coma aggregates have aggregates which are redder, some bluer than the central galaxy. Others have colors that span a range from red to blue.

In Conselice & Gallagher (1998a) the criteria for an object to be an aggregate is defined to be:

1. Primary galaxy must be disk galaxy which is not a dominate member of the cluster.
2. The knots or dwarf galaxies must be asymmetrically distributed and within 2-3 optical radii of the primary.
3. The number of dwarf galaxies, or knots surrounding the primary member must be a statistical excess over the number of similar objects in the cluster field.

Interestingly, we find nine examples of possible galaxy aggregates in the Coma cluster, including the three reported previously in Conselice and Gallagher (1998); however, we find no examples in the other clusters (with the exception of one possibility in AWM 5). These aggregates could in some way be related to the clumping of dwarf galaxies, which we have 10 examples of in Coma, and only four total for the other clusters. Additionally, we find the aggregates to be spread out in the images; that is we do not find an overabundance of this morphology in the densest parts of Coma. If solely a projection effect, caused by the high density of galaxies in this cluster, then we would expect to see more aggregates in the densest part of Coma, however this is strictly not true (see Table 2). Perseus and Abell 2199 also contain an abundant amount of dwarf galaxies, as well as being just as rich as Coma, but have no examples of aggregates. Our failure to see aggregates in these clusters and the other poor AWM clusters suggests that these objects are not mainly in the background.

In this paper we present what are a number of other possible aggregates; these are not as prominent as the three we presented in Conselice & Gallagher (1998), but none the less morphologically qualify as being aggregates. Interestingly, the sizes of the aggregates are all nearly the same, about 20 kpc, which is the size of the tidal diameter for stripping in Coma (Merritt 1984), based on a 100 km s^{-1} velocity dispersion assumption for early type disk galaxies (see Section 7).

4.3. Multiple Galaxies

In our clusters individual galaxies rather frequently appear to be in association with other galaxies, with no apparent interaction occurring. Usually these are in the form of pairs, but

occasionally these types of galaxies are found to be in multiple systems. Classification as a multiple galaxy (MG) further requires that the two or more members must be approximately the same size and apparently close together, with no visible evidence for interactions, in the form of tidal plumes or distortions. Our definition of a multiple galaxy differs from those of Arp (1966) or Zwicky (1957) in that we are not implying a physical association, just an apparent one. Galaxies which are multiple, but show signatures of interactions are classified as interacting galaxies (Section 4.4). Dwarf galaxies which appear to be congregating together are classified separately as dwarf galaxy groups, which will be discussed in Section 4.7. The MG morphological category is the most susceptible to chance superpositions.

Curiously, there is only a slight correlation between galaxy richness and the number of multiple galaxies found. This indicates that some of these systems may be galaxies which are close to one another but are not strongly interacting. They could, for example, be in the early phases of an interaction, before damage is done, or moving at high relative velocities which weakens collisional effects. The color distribution of these systems is shown in Figures 10, 11 and 12. Some of the MG pairs show surprisingly blue colors $(B-R) < 1$, indicating that star formation is probably occurring. It is possible that we are missing some of the finer features of an interaction and are thus misclassifying what should be an interacting galaxy system; suggesting that some multiple galaxies are physical systems. However, the average $(B-R)$ color for multiple galaxies is one of the reddest morphological class (see Table 5), consistent with chance superpositions of non-interacting galaxies accounting for some of this class.

4.4. Interacting Galaxies

Interacting galaxies (IG) are systems which appear to have a disturbed morphology and are in close proximity to another galaxy. For our purposes, close proximity is defined to be two or more galaxies of similar sizes that appear to be within 3 galaxy radii of each other. In some cases, the interaction is fairly obvious for both galaxies; but for others, only one galaxy shows a significant distortion.

If these systems are indeed real, then this would be direct proof of low-velocity galaxy-galaxy interactions in clusters. This category, like the multiple galaxies (MG) is highly subject to chance alignments, but the probability of superimposing two distorted galaxies of similar sizes in a cluster is not high, although possible. Therefore, for a very few cases, we are probably observing a form of low-velocity galaxy-galaxy interaction. Interacting galaxies are also the bluest form of structure, with an average $(B-R) = 1.59 \pm 0.49$, with individual examples with colors $(B-R) < 1$. The blue colors of IG gives a clue to their origins. If these other structures are caused by an interaction with a cluster's gravitational potential, and if any star formation is occurring, it is at a reduced rate as compared with a low-velocity galaxy-galaxy interaction. This could be the result of the

mechanisms which produce the structures being somehow ‘weaker’, but may also be the result of gas stripping occurring prior to tidal interactions, an idea which will be further discussed in Section 7.

4.5. Tailed Galaxies

Galaxies which have a luminous (probably tidal) tail, but no obvious companion, are surprisingly common among our sample, and are likely due in large part to background galaxies (see Section 5). The galaxies in this category have a wide range of sizes, but similar surface brightnesses. Some of these are smaller than the average sized cluster member, with faint tails, facilitating their anonymity until now.

There are abundant examples of tailed galaxies in a variety of different environments that are consistent with several formation scenarios. Tails associated with field galaxies are very common, and are almost always due to interactions between galaxies (e.g. Chromey et al. 1998; Elmegreen et al. 1998). Tidal tails are also locations where dwarf galaxies can form (e.g. Hunsberger et al. 1996), and therefore may be related to the galaxy aggregates. Alternatively, tailed galaxies might be the result of gas stripping in clusters.

Calibrating with our blank field image (Section 2), we find that a significant fraction of the tailed galaxies seen in these clusters are probably due to projection of background galaxies. The galaxies seen in the Hubble Deep Field image are, however, very tiny, and cannot explain the larger galaxies that we find in the clusters that have tails. These tailed galaxies could be interacting with the global potential of the cluster, or could be an interaction with companions which are too small to be detected.

An interaction between two field disk galaxies, which would appear as simply a tailed galaxy when the system is very distant, is not unusual. The interacting galaxies NGC 4038, ‘The Antennae’, and NGC 5996, both consists of a large spiral with one of its arms extended out towards a companion. If very far away, these two galaxies would blend together, and the appearance of these galaxies would be similar to the tailed galaxies seen in our clusters. These galaxies are also possibly morphological similar to the “tadpole” type galaxy found in relative abundance in the Hubble Deep Field (van den Bergh et al. 1996). These “tadpole” galaxies are also isolated and appear to be the result of a distant merger, or from some other dynamical effect. A local analogy of these types of galaxies is possibly NGC 3991⁴, first described by Morgan (1958).

Radio tails attached to galaxies in nearby clusters, including Coma and Perseus are well-known (Feretti et al. 1990; Owen and Eilek 1998), and may have origins related to the optical tailed

⁴NED describes this galaxy as a Magellanic irregular which is involved in an interaction with NGC 3994 and NGC 3995, accounting for its peculiar morphology

galaxies found here. Radio head-tail galaxies are generally found near the core of their clusters, and are thought to originate from ram-pressure stripping with an interaction between the stripped plasma and the ambient gas (Begelman et al. 1979). Tailed galaxies are most common in Perseus, with 0.2 tailed galaxies per arcmin². Interestingly, Perseus is also contains more examples of radio head-tail galaxies than any other cluster (Owen and Eilek 1998). This is another indication that the tail galaxies likely include representatives in clusters, and may point towards an intracluster, ram-pressure event to account for their morphology.

4.5.1. *Debris Arcs*

Debris arcs, like that discovered by Trentham & Mobasher (1998) and the one reported here, are likely to be related to the phenomenon of tailed galaxies. These are luminous bands, thought to consist of stellar tidal debris from galaxies. The debris arc reported in this paper (SA1656-029), has a size of about 20 kpc. These objects, only a few of which are known, are only seen in the Coma cluster. The possible origin of this interesting form of fine-scale substructure is from an interaction with the potential of a cluster, or by some form of galaxy harassment, an idea discussed more in Section 7.

4.6. **Line Galaxies**

Line galaxies with red colors are probably the most unusual, and interesting class of galaxy, which are not known to exist in the field. These are exactly what their morphology indicates. They are extremely thin galaxies which have lengths that are at least 5 times longer than their width. In the field these superthin galaxies probably are extreme late type galaxies seen edge on (e.g. Goad & Roberts 1981; Karachentsev et al. 1993) in which case they are dynamically cold disk systems (Karachentsev & Xu 1991; Matthews & Gallagher 1998). If all line galaxies were superthin extreme late-type systems, then the presence of an excess density of line galaxies towards clusters would be surprising; clusters are generally deficient in late-type spirals. This type of galaxy is also present in our blank field, and a sizable portion of the smaller line galaxies are probably in the background. The bluer line galaxies are likely to be small extreme late type galaxies, Scd-Sdm, seen edge on. Red line galaxies are an oddity, and probably have a different origin.

Of our seven morphological types, line galaxies are the ones that are most likely a normal type of galaxy seen in projection. Possibly, we are seeing a previously unrecognized LSB extreme late-type galaxy component in clusters, which are detected only when they are edge-on and therefore have a higher surface brightness (Bergvall & Rönnbeck, 1995, Dalcanton & Schectman

1996). They could also be a projection effect from a long tailed galaxy, or possible pieces of an arc (Section 4.5.1) seen edge on. Line galaxies, however, present no significant curvature and are much more abundant than the very few examples of arcs as seen in Coma. Also, by far the most abundant location for finding line galaxies is in the Perseus cluster, which has no known examples of galaxy arcs.

A problem with this scenario is the extremely red colors of the line galaxies in Coma have an average color of $(B-R) = 2.18$, a higher average by 0.3 magnitudes than any other fine-scale substructure. Red colors are inconsistent with normal extreme late-type spirals (e.g. Matthews & Gallagher 1997). Because of their red colors, these galaxies might be related to early-type objects within the clusters, or background galaxies seen in projection (Secker et al. 1997). If these are background systems, they are likely to be very thin galaxies seen edge-on. However, we see a significant overabundance of these objects in Perseus, which also has the highest density of tailed galaxies, as compared with the other clusters. Additionally, we find that for Abell 2199 and AWM 5 the line galaxies have average colors near $(B-R) = 1.79 \pm 0.0$ and $(B-R) = 1.42 \pm 0.62$, respectively. The blue colors of line galaxies in AWM 5, and the wide range in colors as seen in Coma (see Figure 16), with some line galaxies having $(B-R) \approx 1$, indicates that a portion of these objects are probably located within these clusters. Redshifts of line galaxies are required to properly resolve this issue.

4.7. Dwarf Galaxy Groups

Excess concentrations of dwarf galaxies in one region define a 'dwarf galaxy group'. These objects usually consist of more than five, mostly small, low surface brightness galaxies in the same region. This type of structure is almost exclusively found in the Coma cluster (Table 3), its origin could be related to the galaxy aggregates, which are also almost exclusively found in the Coma cluster. The tendency for dwarf galaxies to clump together in Coma was originally noticed by Ulmer et al. (1994). Along with multiple galaxies, and galaxy aggregates, the apparent relationship between these galaxies may be due to projection effects. However, a strong argument can be made that some of these structures are real, as they are not found in clusters other than Coma. Coma has a relatively low dwarf galaxy to giant ratio (Secker and Harris, 1996) for its richness, and other clusters like Perseus and Abell 2199 will have the same, or higher dwarf galaxy to giant ratios. Coma, therefore does not have a higher fraction of dwarf galaxies than other rich clusters, and hence there is no reason why we should see more clumping of these dwarf galaxies, if the effect is solely one of projection. The fact that we see only one dwarf galaxy group in Perseus, and only two in Abell 2199, as opposed to the 10 we see in Coma indicates that these objects are most likely real associations. The number density of dwarfs in dwarf groups is around 49 galaxies arcmin^2 . The average number density of similar, or brighter galaxies in other areas of Coma is 5 galaxies arcmin^2 . These systems have densities 20σ above the mean cluster level, and hence are

almost certainly real physical systems.

5. FIELD GALAXY CONTAMINATION

When studying any group of astronomical objects where distances to the objects cannot be known with certainty, one must consider, and correct for, the possibility that some of the objects under study are either in the foreground or background of the system you are trying to study. This is a long standing problem in galaxy cluster research, and is particularly troublesome for the work presented in this paper. However, there are several tests we can perform to determine whether or not what we are observing in these clusters are statistically likely to be part of the cluster, or in the foreground or background.

A large portion of the smaller galaxies in our sample could be the result of projections of background galaxies mixing with and contaminating our samples, and this is a likely origin for the fainter, red objects. Assuming that the Universe, and hence background objects are isotropically distributed, then if our fine-scale substructures are entirely of non-cluster origin, we should see similar proportions in every field. That we do not, and the fact that we see more structures in the richer and closer cluster fields implies that at least some of the features we are seeing are real (Tables 2 & 3). To test this further, we can use an image of a blank area of the sky to determine if any of the structures we are seeing are present in an area which contains no clusters.

To determine a lower limit to contamination, we imaged the Hubble Deep Field (HDF) at the same exposure times used for all of our cluster images (600s). This area was chosen for its lack of any bright stars or galaxies, or galaxy clusters (William et al. 1996) to determine how many of our tiny background galaxies may be due to contamination from distant and small field galaxies. Performing a similar type of analysis that we did on the cluster images, we find four examples of what we would have classified as tailed galaxies, one possible multiple galaxy, two line galaxies, and one distorted galaxy. Naturally, objects like multiple galaxies, and dwarf groups are prone to chance superpositions among cluster members, and this cannot be tested by using the HDF image, but we can compare the non-associated structures. We find no examples of interacting galaxies in the HDF images, but on average we find three per WIYN field in the cluster images. The HDF images have one distorted galaxy, whereas we find seven on average for our cluster fields; distorted galaxies are probably components of the clusters.

However, we do not find this to be true for the line and tailed galaxies. We find an average of 2.5 line galaxies per cluster field as compared to the two found in the blank HDF field. We also find an average of 5.3 tailed galaxies per cluster field as compared to the four seen in the blank field. This indicates that these galaxies might be solely background objects. However, as will be seen, some of these objects are found in large abundance in certain clusters, as well as having peculiar trends in color (see Section 4.5), creating difficulty with a purely background explanation.

Additionally, the HDF tailed galaxies are very small, with barely discernible tails; some tailed galaxies in our sample have similar sizes, but others are very prominent. Future observations using HST images should clarify the morphologies of these galaxies. The line galaxies in the HDF field likewise are morphologically the smallest and faintest. No galaxy aggregates, dwarf groups, or interacting galaxies were observed in the blank field.

The best, and most accurate way to determine if a galaxy is in a cluster is to know its redshift. Unfortunately, we do not have redshift information for the majority of the galaxies in our sample. However, a few of the galaxies in our sample do have known published redshifts, mostly in the Coma cluster. Published redshift studies of the other clusters are disappointingly meager. The galaxies for which redshifts were available from NED⁵ are shown in Table 11.

We find 21 galaxies in the Coma cluster in our catalog can be identified with a redshift, one with Perseus, and four for A2199, and 1 with AWM3. Most of these galaxies, the only ones that we can confirm a redshift for, have velocities which are consistent with cluster membership; with most galaxies having velocities less than 1σ of the cluster velocity dispersion. However, a few exceptions must be noted and may give clues as to the nature of some of the other galaxies in our catalogs. In the Coma cluster the galaxies, SA1656-018, SA1656-026, SA1656-030 have recession velocities $cz = 18300, 48108$, and 35268 km s^{-1} respectively (Table 11). The average Coma velocity is 6917 km s^{-1} ; these objects are in the background and their morphologies are DG, MG, and MG. They also appear very small in our images, similar to the galaxies in our blank field image. Note that SA1656-057, a tailed galaxy, has a recessional velocity of 6629 km s^{-1} , only 288 km s^{-1} different from the average Coma velocity, and certainly a member of the cluster. Also, the line galaxy SA1656-071 has $cz = 8135$, which is within 1σ of the mean cluster velocity, and hence also part of the cluster. Therefore, we can be sure that at least one example of a tailed and line galaxy exist in the Coma cluster, and are not background objects.

We can further test membership of the galaxies by taking the averages of the Coma galaxies in our sample that have known radial velocities, excluding the three obvious background galaxies (SA1656-019, SA1656-026, SA1656-030). The average velocity of these 18 Coma galaxies is $7196 \pm 1726 \text{ km s}^{-1}$, which is close to the value $6917 \pm 47 \text{ km s}^{-1}$ found with a complete sample of 552 redshifts of spectroscopically confirmed members (Colless & Dunn 1996). While obviously not proof that the majority of the galaxies in our catalog are part of their respective clusters, it does show that in Coma, the fine-scale substructure is distributed in velocity space in a similar manner as the average Coma galaxy. The other six galaxies with fine-scale substructures and velocity measurements in A2199, Perseus and AWM3, all have velocities within 1σ of the cluster mean. Also, if our fine-scale substructures are purely background objects, then these should be distributed nearly randomly on the sky. We however, do not see this type of behavior when we plot the positions of our objects (Figures 2 and 3, see next section).

⁵The NASA/IPAC Extragalactic Database (NED) is operated by the Jet Propulsion Laboratory, California Institute of Technology, under contract with the National Aeronautics and Space Administration.

We therefore conclude that our sample probably contains a significant fraction of objects in, or near their respective clusters.

6. RESULTS

6.1. Spatial Distributions

In each of our cluster fields, we find some forms of fine-scale substructure. The denser clusters, e.g. Coma and Perseus, have more examples than the poorer AWM clusters. One of the ways to determine the nature and possible origin of these structures is to find how they vary with local environmental conditions. If we find that the objects are evenly distributed, clumped, or only present in some parts of the clusters, this can give us information concerning the physical nature of these objects.

Figure 3 shows the location as a function of R.A. and Dec. (J2000) for the fields IC 4051, NGC 4881, AWM5, AWM3, NGC 6166, and for the Perseus cluster. Figure 2 shows the six Coma fields (see Table 1). It appears that for most of the fields a form of clumping is occurring, although it is not a significant or outstanding feature. It is rare, even in the low density fields, to find a structure that does not have another one nearby. Also, for some fields, particularly Coma 3, Abell 2199, and Perseus there appear to be voids where no fine-scale substructures are found. This is also hinted at in the various other cluster fields. These void areas do not always, but sometimes contain the larger ellipticals in the cluster.

There are a few more important points worth mentioning concerning the distribution of these structures. In general, the structures seem to be more abundant in richer fields (e.g. Coma, Perseus) than in the poorer clusters (AWM 3 & 5), showing a possible fine-scale substructure density relation. Our structures also tend to avoid the areas around the central galaxies. However, this could be the result of selection bias. Since these structures are not isolated but tend to clump together, this may indicate that in-fall events are occurring into the cluster not as isolated galaxies, but as groups (Henriksen & Byrd 1996).

6.2. Relative Frequencies of Structures

We can learn more about fine-scale substructures by examining the relative numbers of each structure in our five clusters. Tables 2 and 3 show the number of different morphologies as found in each of our five clusters. We can then use this information to investigate the morphological

trends in our clusters. Figures 4 - 6 show the relative distributions of the structures in the six Coma fields (Figure 4), the other two Coma fields surrounded by NGC 4881, and IC 4051, and the fields for Perseus, Abell 2199, AWM 3 and AWM 5 are shown in Figure 5. The total Coma distributions is shown in Figure 5.

To study the salient features of the distributions we can categorize everything into two broad subgroups: galaxy associations (includes AG, MG, dwG) and structures that show either a distortion or interaction (includes DG, IG, TG, and LG). We place every fine-scale substructure into one of these categories, and define Γ to be the ratio of the number of disturbed structures to the number of associations. When we do this, we find that our clusters fall into two broad types: clusters that have their fine-scale substructure dominated by associations, and ones that do not. A high value of Γ , which in our case, would be $\Gamma \approx 10$, would signify a cluster dominated by associations, while a $\Gamma \approx 1$ would be a cluster dominated by disturbed structures. Table 4 shows the values of Γ along with the number of association and disturbed structures. Coma, Abell 2199, and AWM 5 all have Γ values near 1, while Perseus and AWM 3 have Γ values near 10.

Why would some clusters appear to be overabundant in associations, while others are not? There is no obvious answer to this, but we propose that the value of Γ gives a rough indication of the recent dynamical history of a cluster.

We can further see this subdivision of cluster by examining the histograms for the different clusters. The clusters that have a low Γ (Coma, Abell 2199, and AWM 5) all have similar distributions of types of structures (Figures 5 & 6). Multiple galaxies are the most common type of structure in all three of these clusters, with almost identical histograms for A2199 and Coma. In addition, all but one of the dwarf galaxy groups are in these three clusters. On the other hand, for our $\Gamma \approx 10$ clusters, we have very few multiple galaxies (AWM 3 & Perseus; see Figure 6). Both clusters are also dominated by distorted galaxies and tailed galaxies. Therefore, the two types of clusters in our sample have both similar values for Γ as well as similar distributions of structures.

6.3. Magnitudes and Colors

A powerful method of deciphering the origin of these fine-scale substructures is to investigate their colors and their magnitudes. We are able to perform photometry to obtain the colors and magnitudes of the fine-scale substructures in the three clusters: Coma, Abell 2199, and AWM 5. The Perseus images were taken with the WIYN CCD in the fall of 1996 when the CCD was not linear, and we only have one R-band image for AWM 3. Photometry is performed on the R and B images, using only an aperture size of a few pixels at the center of our galaxy. The magnitude and color information presented here is only for the core of each object. Typically the colors of the fainter features, such as tidal tails and distorted parts of the galaxies that are of low surface brightness, cannot be computed with any accuracy with our relatively shallow survey imaging.

When a particular morphological structure has more than one galaxy, such as multiple galaxies, dwarf groups and galaxy aggregates, we measure the brightest member.

Figure 7 shows the color-magnitude diagram for all fine-scale substructure object in the Coma cluster. While this plot has a large scatter, we can still pick up some trends. The color-magnitude diagram shows a very slight trend towards bluer colors at fainter magnitudes with a large scatter. In clusters, it is not surprising to find a color-magnitude diagram with this type of weak correlation. Secker et al. (1997) find a similar type of relationship for Coma dwarf elliptical galaxies. This diagram includes both the large galaxies in our sample, as well as the fainter dwarf galaxies which constitute a part of the sample. It also contains the inevitable background galaxies. Overall, however, there is a pattern at the faint and bright ends of the diagram; objects which have a magnitude brighter than $R = 18.0$ have colors greater than $(B-R) = 2$. However, for the objects with R fainter than 23, nearly every object is bluer than $(B-R) \approx 2$.

We do not see similar color-magnitude diagrams for the clusters Abell 2199, and AWM 5 (Figure 8 & 9). In these two clusters, most of the objects have similar colors, which do not show a dependence on the magnitude. It is possible that we do not pick up the same slight dependence on magnitude that we see in Coma because we do not have enough structures in those clusters to detect any correlations.

By looking at the colors of the individual fine-scale substructures in our clusters, we might be able to better understand the origin of these objects. Figures 10, 11, and 12 show $(B-R)$ scatter plots as a function of the morphological type for our three clusters with color information. For Coma, the average colors for the galaxy types are, from bluest to reddest (see Table 5): Interacting galaxies $(B-R) = 1.62 \pm 0.42$, tailed galaxies $(B-R) = 1.67 \pm 0.65$, distorted galaxies $(B-R) = 1.68 \pm 0.76$, galaxy aggregates $(B-R) = 1.72 \pm 0.51$, dwarf galaxy groups $(B-R) = 1.73 \pm 0.45$, multiple galaxies $(B-R) = 1.90 \pm 0.59$, and line galaxies $(B-R) = 2.18 \pm 1.4$. With the other examples from Abell 2199 and AWM 5, we find that the average colors of these structures throughout all three clusters with photometric information are: Interacting galaxies $(B-R) = 1.59 \pm 0.49$, Tailed galaxies $(B-R) = 1.69 \pm 0.97$, distorted galaxies $(B-R) = 1.71 \pm 0.73$, galaxy aggregates $(B-R) = 1.73 \pm 0.43$, dwarf galaxy groups $(B-R) = 2.10 \pm 0.61$, multiple galaxies $(B-R) = 1.90 \pm 0.61$, and line galaxies $(B-R) = 1.91 \pm 1.0$ (see Table 5).

The bluest objects are the interacting galaxies and tailed galaxies. For interacting galaxies, this is not surprising and is what we would expect if new stars were being formed from the disturbed galaxies undergoing an interaction. However, this is not an extremely blue color, and as can be seen from Figures 10, 11 and 12, a large spread of colors exists for distorted galaxies; some have a color $(B-R) < 1$, while others have $(B-R) > 2.5$. It is impossible to tell from our photometry what the origin of such a wide scatter is for these and the other fine-scale substructures. Several possible scenarios (see Section 7), various degrees of $H\alpha$ emission, and likely background contaminations could be producing this wide scatter.

The next bluest type of fine-scale substructure are the tailed galaxies. These objects are

less prone to projection effects, since the objects consist of only one galaxy, but contaminating background galaxies are likely. A (B-R) color of 1.69 is not very blue, although like the distorted galaxies, the scatter ranges from blue colors (B-R) ≈ 0 , to very red ones (B-R) ≈ 3.5 . If tailed galaxies originate from an intracluster medium interaction followed by a tidal interaction, star formation does not necessarily have to occur. When ram-pressure stripping occurs in a galaxy in-falling into the cluster, it will be stripped of all its gas. Later, when gravitational, or other perturbing forces act on the galaxy, the material that we see as a tail could be old stellar material, with no star formation occurring due to a lack of gas. However, we do have some examples of extremely blue, and also extremely red tails in our sample. These objects may be the result of a form of star formation. Similar arguments can be made for the other structures as well, all of which have a wide scatter in their (B-R) colors (see Figures 16, 17 and 18 for histograms).

As expected, if the structures we are seeing are real, the average colors of the associated objects (AG, dwG, and MG) are all redder than the disturbed structures (IG, TG, DG) with the interesting exception of the line galaxies (LG). The line galaxies are the reddest objects in the Coma cluster (but the bluest in AWM 5), and have the second highest (B-R) color. The color of these objects in Coma are red enough that they could be considered to be background objects in the Coma cluster (Secker et al. 1997). However, the moderate and bluer colors of these objects in Abell 2199 and AWM 5 suggests that this simple interpretation might not fully explain the Coma line galaxies (see Section 4.5, for a full discussion).

Figures 13, 14 and 15 show the distributions of magnitudes for our sample as a function of morphology. There is a wide scatter of magnitudes, with some interesting features. The line galaxies in all three clusters have the faintest magnitudes. In Coma, the brightest line galaxy has a central magnitude of about 20.5, which for most of the other structures, the brightest central magnitude is around 16.5. This is an indication of the low surface brightness nature of these objects, as well as the violation of the “fainter-bluer” relation found by Secker et al. (1997) for Coma dwarf elliptical galaxies. Figures 19, 20 and 21 show histograms of the magnitudes of the fine-scale substructures found in our three clusters. We do not see a rise in the number of galaxies, for any morphology at fainter magnitudes. Additionally, the dwarf galaxy groups (dwG) have similar magnitudes and much less of a spread as compared with the other features. The features with the largest spreads in magnitudes are the distorted galaxies and the multiple galaxies. The other features with low surface brightness are the interacting galaxies and tailed galaxies; however there are examples within these classes that have high surface brightness features.

7. ORIGINS OF STRUCTURES

The structures that we see in these clusters have a few possible origins. They could be due to superpositions of background galaxies (Section 5), causing us to think that a particular

galaxy is part of the cluster. This is certainly the case for some of our galaxies, but our failure to observe similar abundances of structures in our control field, and the relative increase in density of the structures in the fields of denser clusters, as compared with the density in the poorer clusters, as well as confirmed membership for 89 % of the galaxies with known redshifts all show that a significant fraction of our catalog are cluster members (see Section 5 for a more detailed discussion). Furthermore, with the caveat that some of our catalog is certainly of background origin, we will hereafter assume that each of our morphological classes (AG, TG, DG, MG, LG, IG, dwG) have representatives in galaxy clusters.

The Coma cluster contains a significant number of blue galaxies (e.g. Bothun & Dressler 1986; Caldwell et al. 1993) which resemble Butcher-Oemler galaxies as seen in distant clusters (Butcher & Oemler 1978, 1984). We further confirm this observation, by finding a significant fraction of galaxies in our sample with blue colors. In fact, almost every morphological class has objects with colors near $(B-R) \approx 1$. However, for the most part, the structures we find have moderate to fairly red $(B-R)$ colors, and hence are dissimilar in this respect to distant B-O galaxies. All of the galaxies in our sample are similar to B-O galaxies in that they have distorted morphologies. Since some of our sample is blue, with the rest red, and B-O galaxies are both distorted and blue, this indicates that another mechanism is probably producing the red galaxies. However, based on previous observations of blue Coma galaxies (e.g. Caldwell et al. 1993), and the results presented here, processes that produce the blue galaxies in our sample are probably similar to those occurring in the B-O clusters.

Four basic models predict how structures might have formed; low-velocity galaxy-galaxy interactions, gas stripping, and tidal interactions with the cluster potential. The fourth option, 'galaxy harassment' combines interactions with the cluster's gravitational potential with collisions with galaxies in the cluster. From our color information, we know that some of the structures in our catalogs have colors that are consistent with very little active star formation, so starbursts alone cannot produce the observed effects, although they are a likely factor in the bluer galaxies. These blue galaxies have been observed previously in Coma (Caldwell et al. 1993), and are interpreted as star forming galaxies in the cluster. Several models have been developed which predict how star formation within a galaxy will behave during its in-fall into a rich cluster, which we will also discuss.

7.1. Gas Stripping

If hierarchical structure formation is occurring in clusters, then galaxies should be accreted by the cluster, slowly building up the cluster's mass. If these galaxies are field disk galaxies falling into a cluster, then a large portion of their gas may be stripped into the cluster environment by a variety of processes (Dressler & Gunn, 1986; Gunn & Gott 1972; Valluri & Jog 1990, 1991). If this

is occurring, it will eventually lead to disk galaxies in the cluster which are devoid of significant amounts of gas, potentially converting spirals into S0 galaxies. This model is supported by the lack of H α emission from late-type spirals in the Coma cluster (Moss & Whittle 1997), and other observations of gas deficiencies in cluster spirals (e.g. Haynes & Giovannelli 1986). If all the gas is stripped out of a disk while it enters the cluster, then tidal forces will be unlikely to create a star formation event, as the necessary raw materials are absent.

If ram-pressure is occurring, it could happen on a much faster time scale than other mechanisms which produce tides and distortions in an in-falling galaxy. Soon after falling into a rich cluster, which typically have intracluster mediums extending significantly away from the core of the cluster, gas will be removed from the galaxy into the intracluster medium. This may occur quickly before any other mechanism will have had time to produce an effect on the in-falling galaxy. During this stripping of gas, the galaxy will start an orbit inside the cluster. While on this orbit mechanisms such as low-velocity galaxy-galaxy interactions (Section 7.2) or galaxy harassment (Section 7.3) will begin to strip the galaxy dynamically. Usually when dynamical stripping of a galaxy occurs, the gas inside is compressed and new stars are formed. However, since the in-falling galaxy has had its gas stripped by the intracluster hot gas, no material is available to produce any new stars. Therefore, the stripped material only contains the old stellar populations which existed before the galaxy was accreted by the cluster. Thus, galaxies which look distorted, but have red colors are produced.

Ram-pressure stripping may also cause some forms of star formation in an in-falling galaxy, however the specifics of such a process remain somewhat uncertain (Henriksen & Byrd 1996).

7.2. Low-Velocity Galaxy-Galaxy Interactions

Low-velocity galaxy-galaxy interactions are traditionally popular mechanisms for explaining the B-O effect as seen in distant clusters (Lavery & Henry 1988, 1994). In the field, it is fairly common to observe low-velocity galaxy-galaxy interactions, most of which cause some form of star formation in the galaxies undergoing an interaction. Galaxy interactions can also explain many other features of unusual galaxies, including morphological changes without associated star formation.

We also find in our nearby cluster images what appear to be examples of galaxies which are interacting. These morphological interacting galaxies are, however, one of the rarer classes of structures in our catalogs: we find about twice as many distorted galaxies - disturbed galaxies without an obvious companion. Additionally, some morphologically selected interacting galaxies could be superpositions of two slightly abnormal galaxies. Hence, low relative velocity pairs with obvious signatures of interactions are rare. However, for a few cases, noted in the catalogs, there are systems undergoing a rather obvious interaction, which are also members of their respective

clusters. These galaxies typically have blue colors.

The best way to determine if two galaxies are physically interacting, is to know the radial velocity of each member of the pair. A high velocity difference would probably indicated that the mechanism for producing the disturbed morphology is something other than an interaction between the two galaxies, at least as envisioned by Toomre and Toomre (1972). One of our interacting pairs, SA1656-065 (Markarian 60), has a velocity difference of 4000 km s^{-1} . This velocity difference is too high for this to be a standard low-velocity galaxy-galaxy interaction. However, other more convincing cases than SA1656-065 are found, even though we do not always have redshift information for these.

A likely candidate for a low-velocity galaxy-galaxy interaction is in AWM 3, where the central galaxy NGC 5629 shows evidence of ripples or shells, which point in the direction of an elongated galaxy IC 1017. The redshifts for these objects are 4498 km s^{-1} and 4382 km s^{-1} , respectively, a velocity difference of only 116 km s^{-1} . This is small enough to allow a strong interaction between these two galaxies to occur. Other possible examples exist, and can be confirmed once their radial velocities are known. We therefore conclude that low-velocity galaxy-galaxy interactions in clusters probably do take place, but are not a dominate effect in our sample (see Table 3).

Interacting galaxies are also the bluest form of structure in our survey. A low-velocity galaxy-galaxy interaction has a much shorter time scale than an interaction between a galaxy and the cluster potential, and is more likely to occur in a group in the early stages of infall. Therefore, this class of interaction can occur before ram-pressure stripping depletes the neighboring galaxies of their gas new stars are created from. Each low relative-velocity, physically interacting galaxy pair thus is a likely candidate for being in the the early phases of in-fall on the periphery of the cluster.

7.3. Tidal forces from cluster potential and Galaxy Harassment

Tidal interactions between the cluster gravitational potential and a member galaxy was considered in detail by Merritt (1983, 1984), and applied to disk galaxies by Valluri (1993). In the scenario presented in these papers, a galaxy begins to undergo tidal stripping when it falls into a cluster. The outer portions of this in-falling galaxy are dynamically heated and possibly stripped away from the remainder of the galaxy, potentially producing a change in morphology of the in-falling galaxy. The radius of the in-falling galaxy to where this stripping occurs, called the tidal radius, depends upon the in-falling galaxies velocity dispersion v_g and that of the cluster v_{cl} . The *minimum* tidal radius r_T of the in-falling galaxy occurs for objects near the cluster core radius, R_c , given by:

$$r_T = R_c \frac{1}{2} \frac{v_g}{v_{\text{cl}}}.$$

As shown in Conselice and Gallagher (1998), the star knots or dwarf galaxies for RB 55 and RB 60 are located at about the tidal radius for Coma. The other aggregates found in Coma, are also of similar size. Therefore, at least these objects could be direct results of tidal stripping caused by the cluster gravitational potential.

Other aspects of tidal stripping within rich clusters have been considered as possible mechanisms for the production of active and barred galaxies in clusters (Byrd & Valtonen 1990; Henriksen & Byrd). These models predict that in-falling disk galaxies will produce significant starbursts, especially near the cluster core; this, of course, is based on the survival of sufficient amounts of gas in the inner disks.

Another method of producing disturbances in cluster galaxies is to consider a combination of effects which lead to 'galaxy harassment.' The models for galaxy harassment, developed by Moore and collaborators (Moore, Lake & Katz 1998; Moore et al. 1996a, Moore et al. 1996b) present a natural explanation for some of our structures. Galaxy harassment occurs when a galaxy experiences weak encounters from bright cluster galaxy members, and is subject to tidal forces, as discussed earlier. The tailed galaxies and aggregates could be the direct result of in-falling galaxies which are currently undergoing a form of "morphological transformation" via harassment that produces the distorted structures.

In the model by Moore et al. (1998), disk galaxies orbiting a virialized cluster are slowly transformed from disk galaxies, as seen in higher z clusters, to dwarf spheroidal systems that are abundant in nearby rich clusters (e.g. Secker & Harris, 1996). On the way to becoming a spheroidal system the galaxies undergoing harassment develop tidal tails composed of the material in the galaxy, both stars and gas, and will contribute to the general intracluster medium. One particularly interesting effect of galaxy harassment, as shown dramatically in the video accompanying Moore et al. (1998), is the production of long tidal tails. This may be the most natural explanation for the occurrence of galaxy arcs and tidal tails as seen in Coma, which are morphologically similar to the harassment simulations. Galaxies that are most prone to undergoing this type of transformation are low density, low mass galaxies that have orbits that take them close to the cluster core. If the galaxy in-fall process is an ongoing one, then the tailed galaxies we see could be the result of this in-fall occurring at the present time. Additionally, galaxy harassment allows for galaxies which are not in the core of the cluster to become distorted, an effect that we see in our images, where fine-scale substructures occur outside of the cores of the clusters.

Some of the galaxy aggregates (Conselice & Gallagher, 1998) could also be the result of galaxy harassment, or any mechanism that produces tidal tails. A disk galaxy falling into the core of a rich cluster like Coma (where almost all galaxy aggregates are found) will experience harassment, or some form of cluster interaction, and as a result will develop tidal tails as proposed by Moore

et al. (1998), Byrd and Valtonen (1990) and Merritt (1985). If the tidal stripping is sufficient enough to propel enough material from the disk galaxy, dwarf galaxies could in principle form in the debris, creating a galaxy aggregate.

Models where dwarfs are created from galaxy interactions (Zwicky 1956; Barnes & Hernquist 1992) and observations of dwarfs in tidal tails (Yoshida et al. 1994; Hunsberger et al. 1996), support, in principle, this possibility. In addition the knots surrounding the aggregates RB 55 and RB 60, both located in the Coma core, have absolute magnitudes ranging from -12 to -14, which with fading would overlap the magnitudes of local dwarf spheroidal systems (Conselice & Gallagher, 1998). However, before this possibility could be entertained further, the true physical nature of the aggregates based on spectra, including redshifts, as well as further modeling, is necessary.

Our data suggest that interactions with the gravitational potential of a cluster via harassment, or gas stripping are probably the dominate physical mechanisms for the creation of fine-scale substructures in nearby clusters. The observations of isolated distorted and tailed galaxies evidently are not explained by low-velocity galaxy-galaxy interactions, and the few possible low-velocity galaxy-galaxy interactions that we do see could result from pairs and groups undergoing tidal compression as they enter the cluster.

8. CONCLUSIONS

We have performed a purely morphological and photometric study of unusual fine-scale substructures in five nearby clusters (Coma, Perseus, Abell 2199, AWM 5 and AWM 3); placing all observed structures into seven different categories. These morphological categories are: Interacting galaxies (IG), distorted galaxies (DG), tailed galaxies (TG), line galaxies (LG), multiple galaxies (MG) and dwarf galaxy groups (dwG) (see Fig. 1).

Our photometric information indicates that for most of the galaxies in our catalogs the central (B-R) colors have normal distributions with some galaxies having extremely blue, $(B-R) \approx 0$, or extremely red colors $(B-R) \approx 3.5$. While a minority of structures are associated with some form of a starburst, others are probably quiescent, perhaps due to a lack gas, and still others are of background objects.

By examining the relative distributions of structures, we classify the galaxy clusters in our sample into two types: those that are dominated by apparent galaxy associations (dwarf groups, multiple galaxies, galaxy aggregates), and those that have very few associations, relative to distorted structures. We define a factor Γ to be the ratio of distorted structures (interacting galaxies, distorted galaxies, tailed galaxies, line galaxies) to apparent galaxy associations (dwarf groups, multiple galaxies and galaxy aggregates). We find the value of Γ to be either close to 1 for association dominated clusters (Coma, Abell 2199, and AWM 5), and about 10 for non-association

dominated clusters (Perseus and AWM 3). We further propose that Γ may be related to the viralization status, or is a measure of the recent galaxy in-fall rate into a cluster.

We show that structures have a clumpy appearance and avoid the areas occupied by the cD galaxies in the rich clusters. Since distorted structures tend to cluster together, this may be an indication that in-falling galaxies are entering galaxy clusters as members of galaxy groups. We further find that the bluest structures of our seven categories are the distorted, interacting and tailed galaxies, which is what one would expect if these features are cluster members.

Based on models, and the overabundance of structures that appear to be isolated from nearby companions, we conclude that the mechanisms producing these fine-scale substructures are interactions through the cluster potential, via galaxy harassment (Moore et al. 1998), or by tidal stripping (Merritt 1984; Henriksen & Byrd 1996). The implication is that tides and interactions in clusters are an important component of nearby galaxy cluster evolution. These features are fairly common in nearby clusters and are not solely the providence of distant clusters. Furthermore, these features must be considered and accounted for in any future attempts to understand the structure and evolution of nearby clusters.

C.J.C. thanks members of the astronomical community for their suggestions and encouragement during his poster presentation on this topic at the January 1998 AAS meeting in Washington D.C. (Conselice & Gallagher, 1997). We thank F. Schweizer and K. Strobach for useful comments and suggestion on a draft of this paper. We also thank the referee for their suggestions which improved and clarified several important points. We also thank B. Otte for help with the observations. This work was supported in part by the National Science Foundation through grant AST-980318.

REFERENCES

Albert C.E., White R.A. & Morgan W.W. 1977, *ApJ*, 211, 309
Arp H. 1966, *ApJS*, 14, 1
Arp H. & Madore B.F. 1987, 'A Catalogue of Southern Peculiar Galaxies and Associations, Vol. I Positions and Descriptions', Cambridge: Cambridge University Press)
Bahcall N.A. 1980, 238, 117
Barnes J.E. & Hernquist, L. 1992 *ARA&A*, 30, 705
——— 1992, *Nature*, 360, 715
Barnes J.E. 1997 in Galaxy Interactions at Low and High Redshifts, IAU Symp. 186, ed. D.B. Sanders, p.36
Bautz M.P. & Morgan W.W. 1970, 162, 149

Beers T.C. & Geller M.J. 1983, *ApJ*, 274, 491

Beers T.C., Geller M.J., Huchra J.P., Latham D.W., & Davis R.J. 1984, *ApJ*, 283, 33

Begelman M.C., Rees M.J., & Blandford R.D. 1979, *Nature*, 279, 770

Bergvall N. & Rönnbeck J. 1995, *MNRAS*, 273, 603

Bothun G.D. & Dressler A. 1986, *ApJ*, 301, 57

Bridges T.J., Carter D., Harris W.E. & Pritchett C.J. 1996, *MNRAS*, 281, 129

Briel U.G., Henry J.P., & Boehringer H. 1992, *A & A* 259, L31

Butcher H. & Oemler A, Jr. 1978, *ApJ*, 219, 18

——— 1984, *ApJ*, 285, 426

Byrd G. & Valtonen M. 1990, *ApJ*, 350, 89

Caldwell N., Rose J.A., Sharpless R.M., Ellis R.S., & Bower, R.G. 1993, *AJ*, 106, 473

Chromey F.R., Elmegreen D.M., Mandell A., & McDermott J. 1998, *AJ*, 115, 2331

Colless M. & Dunn A.M. 1996, *ApJ*, 458, 435

Conselice C.J. 1997, *PASP*, 109, 1251

Conselice C.J. & Gallagher J.S. III 1997, *BAAS* 191, 106.9

——— 1998a 1998, *MNRAS*, 297, L34

——— 1998b, in prep

Couch W.J., Ellis R.S., Sharples R., & Smail I. 1994, *ApJ*, 430, 121

Crone M.M., Evard A.E. & Richstone D.O. 1996, *ApJ*, 467, 489

Currie M.J. 1983 in Clusters and Groups of Galaxies, ed. F. Mardirossian, G. Giuricin., M. Mezzetti (D. Reidel Publishing: Dordrecht)

Dalcanton J.J. & Shectman S.A. 1996, *ApJ*, 465, L9

Davis D.S. & Mushotzky R.F. 1993, *AJ*, 105, 409

Dressler A. & Gunn J.E. 1983, *ApJ*, 270, 7

——— 1990, in Evolution of the Universe of Galaxies, ed. R. Kron (New York: PASP), 200

Dressler A., Oemler A. Jr., Butcher H., & Gunn J.E. 1994, *ApJ*, 430, 107

Dressler A., Oemler A. Jr., Couch W.J., Smail I., Ellis R.S., Barger A., Butcher H., Poggianti B.M., & Sharples R.M. 1997, *ApJ*, 490, 577

Dutta S.N. 1995, *MNRAS*, 276, 11

Elmegreen D.M., Chromey F.R., Knowles B.D., & Wittenmyer R.A. 1998, *AJ*, 115, 1433

Feretti L., Dallacasa D., Giovannini G., & Venturi T. 1990, *A&A*, 232, 337

Fisher D., Illingworth G., & Franx M. 1994, *AJ*, 107, 160

Fitchett M. & Webster R. 1987, 317, 653

Forman W. & Jones C.J. 1982, ARA&A, 20, 547

Gaetz T.J., Salpeter E.E. & Shaviv G. 1987, ApJ, 316, 530

Gallagher J.S., Han M. & Wyse R.F.G. 1997, in Dark and Visible Matter in Galaxies, PASP Conf Ser 117, eds. M. Persic & P. Salucci, p66

Gallego J., Zamorano J., Rego M., Alonso O., & Vitores A.G. 1996, A&AS, 120, 323

Girardi M., Escalera E., Fadda D., Giuricin G., Mardirossian F., & Mezzetti M. 1997, ApJ, 482, 41

Gunn J.E. 1987, in Nearly Normal Galaxies, ed. S.M. Faber (New York:Springer Verlag), p. 455

Gunn J.E. & Gott J. R. 1972, ApJ, 176, 1

Haynes M.P., Giovanelli R. 1986, ApJ, 306, 466

Henriksen M.J. & Byrd G., 1996, ApJ, 459, 82

Henriksen M.J. 1985, Ph.D. thesis, University of Maryland

Hoessel J.G. 1980, ApJ, 241, 493

Hunsberger S.D., Charlton J.C., & Zaritsky D. 1996, ApJ, 462, 50

Icke V. 1985, A&A, 144, 115

Johnson M.W., Cruddace R.G., Fritz G., Schulman S., & Friedman H. 1978, ApJL, 231, L45

Karachentsev I.D., Karachenstseva V.E., & Parnovskij S.L 1993, AN, 314, 97

Karachentsev I.D. & Xu Z. 1991, PAZh, 17, 321

Kauffmann G. 1995, MNRAS, 274, 153

Kenney J.D.P., Koopmann R.A., Rubin V.C. & Young J.S. 1996, AJ, 111, 152

Kenney J.D.P., Rubin V.C., Planesas P., & Young J.S. 1995, ApJ, 438, 135

Kent S.M. & Gunn J.E. 1982, AJ, 87, 945

Koopman R.A. & Kenney J.D.P., ApJL, 497, 75

Kriss G.A., Cioffi D.F. & Canizares C.R. 1993, ApJ, 272, 439

Lake G. & Dressler A. 1986, ApJ, 310, 605

Landolt A.R. 1992, AJ, 104, 372

Lauberts A. 1982, 'The ESO/Uppsala Survey of the ESO(B) Atlas', (Garching:ESO)

Lauer T.R. 1986, ApJL, 311, 34

Lavery R.J. & Henry J.P. 1988, ApJ, 330, 596

——— 1994, ApJL, 426, 524

Lucy J.R., Gray P.M., Carter D., & Terlevich R.J. 1991, MNRAS, 248, 804

Malphrus B.K., Simpson C.E., Gottesman S.T., & Hawarden T.G. 1997, AJ, 114, 1427
Matthews L.D. & Gallagher J.S.III. 1997, AJ, 114, 1899
Mellier Y., Mathez G., Mazure A., Chauvinau B., & Proust D. 1988, A&A 199, 67
Merritt D. 1984, ApJ, 276, 26
Merritt D. 1983, ApJ, 264, 24
Mohr J.J., Fabricant D.G., & Geller M.J. 1994, ApJ, 413, 492
Moore B., Lake G., & Katz N. 1998, ApJ, 495, 139
Moore B., Katz N., Lake G., Dressler A., & Oemler A. 1996, Nature, 379, 613
Moore B., Katz N., & Lake G. 1996, ApJ, 457, 455
Morgan, W.W. 1958, 70, 364
Morgan, W.W., Kayser, S., & White, R.A. 1975, ApJ 199, 545
Nulsen P.E.J. 1982, MNRAS 198, 1007
Oemler A, Jr., Dressler A., & Butcher H.R., 474, 561
Ostriker J.P. & Tremaine S.D. 1975, ApJL, 202, 1
Price B., Burns J.O., Duric N., & Newberry M. 1991, AJ, 102, 14
Pritchett C.J. & Harris W.E. 1990, ApJ, 355, 410
Ramella, M., Geller, M.J., & Huchra, J.P. 1989, ApJ, 344, 57
Rood H.J. & Baum, W.A. 1968, AJ, 72, 398
Sarazin C.L. 1986, Rev. Mod. Phys., 58, 1
Schneider D.P., Gunn J.E., & Hoessel J.G. 1983, ApJ, 268, 476
Secker J. 1998, Private Communication
Secker J., Harris, W.E., & Plummer J.D. 1997, PASP, 109, 1377
Secker J. & Harris, W.E. 1996, ApJ, 496, 623
Siddiqui H., Stewart G.C., & Johnstone R.M. 1998, A&A, 334, 71
Sijbring D. & DeBruyn A.G. 1998, A & A, 331, 901
Slezak E., Durret F. & Gerbal D. 1994, AJ, 108 1996
Strom K.M & Strom S.E. 1978, AJ, 83, 1293
Toomre A. & Toomre J. 1972, ApJ, 178, 623
Toomre A. 1977, in The Evolution of Galaxies and Stellar Populations ed. B.M. Tinsley and R.B. Larson (New Haven: Yale Univ. Observatory), p. 401
Toomre A. 1978, in Large Scale Structure of the Universe, ed. M.S. Longair & J. Einasto (Reidel, Dordrecht), p. 109.

Trentham N. & Mobasher B. 1998, MNRAS (In Press)

Ulmer M.P., Nichol R.C., Martin D.R., Wipf S., Bernstein G., Whittman D., & Tyson J.A. 1994, in ESO/OHP Workshop - Dwarf Galaxies, ed. G Meylan, P Prugniel, 121

van den Bergh S. 1982, PASP, 94, 459

van den Bergh S., Abraham R.G., Ellis R.S., Tanvir N.R., & Santiago B.X. 1996, 112, 359

Valluri M. 1993, ApJ, 408, 57

Valluri M., & Jog C. 1990, ApJ, 357, 367

Vigroux L., Lachieze-Roy M., Thuan T.X., & Vader, J.P. 1986, AJ, 91, 70

Vikhlinin A., Forman W. & Jones C. 1997, ApJL, 474, L7

Wang D.Q. & Ulmer M. 1997, MNRAS, 292, 920

West M. J. 1994, in Clusters of Galaxies, ed. F. Durret, A. Mazure, J. Tran Thanh Van (Gif-sur-Yvette: Editions Frontires), 23

White S.D.M., Briel U.G., & Henry J.P. 1993, MNRAS, 261, L8

Williams R.E., Blaauw B., Dickinson M., Dixon W. V., Ferguson H.C., Fruchter A.S., Giavalisco M., Gilliland R.L., Heyer I., Katsanis R., Levay Z., Lucas R.A., McElroy, D.B., Metro L., & Postman M. 1996, AJ, 112, 1335

Williams B.A., & Lynch J.R. 1991 AJ, 101 1969

Yoshida M., Taniguchi, Y., & Murayama, T. 1994, PASJ 195, 46

Zabludoff A.I., Huchra J.P., & Geller M.J. 1990 ApJS, 74, 1

Zwicky F. 1956, *Ergebnisse d. exakten Naturw.*, 29, 344

Zwicky, F. 1957, *Morphological Astronomy* (Berlin: Springer)

FIGURE CAPTIONS:

Fig 1 — Six examples of the morphological structures discussed in this paper. Aggregate images can be found in the paper Conselice & Gallagher (1998), and are not included here. Each example is typical for the entire sample of our catalog.

Fig 2 — The distributions of fine-scale substructures in the Coma cluster for the first six Coma fields (Table 2). The symbol x marks the location of a structure. In this figure and in Figure 3, it can be seen that the structures tend to congregate together.

Fig 3 — The distributions for the two Coma fields surrounded by NGC 4881 and IC 4051, as well as the distributions in the clusters: Perseus, Abell 2199, AWM 3 and AWM 5. We see similar effects occurring as in the other Coma fields (Fig 2). The structures tend to clump together, with few structures appearing alone, and some in apparent groupings. We can also see 'bubble' shaped structures in these diagrams, especially for the rich fields of Abell 2199, Perseus and AWM5.

Fig 4 — Histogram of structures as found in the six Coma fields. For most fields the dominate type of structure is either the multiple galaxy, or dwarf galaxy group morphology. There is also a dominance of tailed galaxies in these fields of Coma. Coma 1 field is unusual in that it is dominated by interacting galaxies, and not multiple galaxies and tailed galaxies.

Fig 5 — Total Coma histogram with all objects included showing a similar dominance of multiple galaxies and tailed galaxies as seen in Fig. 4.

Fig 6 — Histograms of structures for the two remaining Coma fields, as well as the fields for the Perseus cluster, Abell 2199 and AWM 3 & 5. Here, we can see significant differences in the histogram trends between these clusters and the Coma histogram (Fig 5). The histograms for Coma (Fig 5), Abell 2199, and AWM 5 are similar, and AWM 3 & Perseus are similar to each other. The values for Γ for these clusters, also correlate (Table 4). Coma, Abell 2199, and AWM 5 having $\Gamma \approx 1$, while Perseus and AWM 3 have $\Gamma \approx 10$.

Fig 7 — The color-magnitude diagram for all structures found in the Coma cluster. A very slight correlation between color and magnitude can be seen, with fainter objects bluer. This relation may have origin similar to the one for dwarf ellipticals in Coma found by Secker et al. (1997).

Fig 8 — The color-magnitude diagram for Abell 2199, including all structures.

Fig 9 — The color-magnitude diagram for AWM 5, including all structures.

Fig 10 — The color distributions for each of the morphology types as found in the Coma cluster. The average colors for each morphology is shown in Table 5. Each morphological type shows a wide scatter in color, with most having objects as blue as $(B-R) \approx 1$ and as red as $(B-R) \approx 3.0$. The widest scatter is for the line and tailed galaxies, possibly indicating that the reddest members are background galaxies. Most of the features however have average colors which are slightly bluer than the average Coma galaxy.

Fig 11 — The color distributions for structures in Abell 2199. As with the Coma cluster (Fig 10), we see a wide range in the colors for the individual structures.

Fig 12 — The color distributions for the structures in AWM 5. Like Abell 2199 (Fig 11) and Coma (Fig 10), the distributions span a wide range in color, indicating potentially different origins for some of the structures we are seeing.

Fig 13 — The magnitude distributions for the structures found in the Coma cluster. Like the color distribution (Fig 10), there is a wide range in magnitudes found for each morphology class. Interestingly, the line and tailed galaxies have the faintest magnitudes, and are also the most likely to be of background origin based on blank field comparisons (see text). Galaxy aggregates have magnitudes which span the smallest range in magnitudes with a range of only about 3.5 magnitudes. The multiple galaxies and distorted galaxies span a wide range from 16.5 to 24.5 central magnitudes.

Fig 14 — The magnitude distributions for the structures found in Abell 2199. Like the distributions in Coma (Fig 13), the range for each morphological class is large. Some types, like aggregates and interacting galaxies are not found in this cluster.

Fig 15 — The magnitude distributions for the structures found in AWM 5. As with Abell 2199 (Fig 14) and Coma (Fig 13), there is a wide scatter in each morphological type. With line galaxies and tailed galaxies having the faintest magnitudes, a similar effect seen in the Coma cluster.

Fig 16 — Color histograms for each morphological type as found in the Coma cluster. Most of the histograms have a Gaussian type shape, with exception of the line galaxies.

Fig 17 — (B-R) color histogram for the structures as found in Abell 2199.

Fig 18 — (B-R) color histogram for the structures found in AWM 5.

Fig 19 — Magnitude histograms for the structures found in the Coma cluster. We do not see a Gaussian shape for the histograms, as we do in the color histograms (Fig 16). A wide spread in magnitudes for each type is seen, with the exception of the dwarf groups.

Fig 20 — Magnitude histograms for the structures in Abell 2199, showing a wide range in magnitudes, similar to Coma (Fig 19)

Fig 21 — Magnitude histograms for structures found in AWM 5.

Table 1: Observing Log

ID	Cluster	R.A. (J2000)	Dec (J2000)	filters	Exp. Times	$cz_{cluster}$
Coma1	Coma	12 59 43.1	27 57 44.0	R & B	600s, 900s	6942 km s ⁻¹
Coma2	Coma	12 59 08.0	27 57 49.0	R & B	600s, 900s	6942 km s ⁻¹
Coma3	Coma	12 58 59.1	27 47 30.0	R & B	600s, 900s	6942 km s ⁻¹
Coma4	Coma	12 59 56.0	27 51 60.0	R & B	600s, 900s	6942 km s ⁻¹
Coma5	Coma	13 00 18.0	28 03 00.0	R & B	600s, 900s	6942 km s ⁻¹
Coma6	Coma	12 58 50.0	28 08 00.0	R & B	600s, 900s	6942 km s ⁻¹
NGC 4881	Coma	12 59 57.7	28 14 48.0	R & B	600s, 900s	6942 km s ⁻¹
IC 4051	Coma	13 00 54.5	28 00 26.6	R & B	600s, 900s	6942 km s ⁻¹
PerNR	Perseus	03 19 53.7	41 33 46.0	R & B	600s, 900s	5486 km s ⁻¹
PerS	Perseus	03 19 47.7	41 28 46.0	R & B	600s, 900s	5486 km s ⁻¹
NGC 6166	Abell 2199	16 28 38.0	39 31 05.0	R & B	600s, 900s	9063 km s ⁻¹
AWM 5	AWM 5	16 55 58.0	27 55 47.0	R & B	600s, 900s	10346 km s ⁻¹
AWM 3	AWM 3	14 26 06.0	26 01 13.0	R & B	600s, 900s	4497 km s ⁻¹

Table 2 : Structures in Coma Fields

Field	Cluster	MG	IG	DG	dwG	TG	LG	AG
Coma 1	Coma	0	7	6	1	0	0	1
Coma 2	Coma	1	0	2	3	2	0	0
Coma 3	Coma	13	0	5	1	5	3	0
Coma 4	Coma	2	3	1	0	3	1	2
Coma 5	Coma	5	1	1	2	1	2	2
Coma 6	Coma	3	0	1	2	3	1	1
NGC 4881	Coma	1	0	2	0	5	0	2
IC 4051	Coma	9	0	2	1	2	0	1
Total		34	11	20	10	21	7	9

Table 3 : Number of Structures in Each Cluster (per field)

Field	Cluster	MG	IG	DG	dwG	TG	LG	AG
Coma	Coma	34 (4.3)	11 (5.5)	20 (2.5)	10 (1.3)	21 (2.7)	7 (1)	9 (1.2)
Perseus	Perseus	8 (4)	7 (3.5)	32 (16)	2 (1)	15 (8)	13 (7)	0 (0)
NGC 6166	A2199	10	1	8	2	9	1	0
AWM 3	AWM 3	1	0	5	0	4	0	0
AWM 5	AWM 5	11	4	2	0	3	3	1
Total		64	23	67	14	52	24	10

Table 4: Values of Γ

Cluster	Disturbed Structures	Associations	Γ
AWM 3	9	1	9.00
Perseus	67	10	6.70
A2199	19	12	1.58
Coma	59	52	1.13
AWM 5	12	12	1.00

Table 5: Average Colors of Structures

Morph	Coma	Abell 2199	AWM 5	Total Ave
IG (Interacting)	1.62±0.42	—	1.47±0.84	1.59±0.49
TG (Tailed)	1.67±0.65	1.90±1.28	1.29±1.80	1.69±0.97
DG (Distorted)	1.68±0.76	1.80±0.90	1.51±0.79	1.71±0.73
AG (Aggregates)	1.72±0.51	—	1.73±0.00	1.73±0.42
dwG (Dwarf Groups)	1.73±0.45	3.02±0.87	—	2.10±0.76
MG (Multiple)	1.90±0.59	1.73±0.58	2.01±0.71	1.90±0.61
LG (Line)	2.18±1.40	1.79±0.00	1.42±0.62	1.91±1.00

Table 6: Structures Found in the Coma Cluster

Name	R.A.(J2000)	Dec (J2000)	R	B-R	Morphology	Notes
SA1656-001	12 59 43.5	27 53 35	23.16±0.30	2.24±0.40	MG, IG	Sml, Wispy
SA1656-002	12 59 43.0	27 54 25	23.16±0.20	1.58±0.24	TG	Possible Interaction
SA1656-003	12 59 41.0	27 56 35	22.31±0.10	1.58±0.12	DG	IG?
SA1656-004	12 59 44.1	27 58 17	22.96±0.19	1.663±0.22	dwG	8 galaxies, all D
SA1656-005	12 59 48.0	27 59 40	22.99±0.26	1.986±0.28	MG, IG	one bright, one faint
SA1656-006	12 59 52.0	27 59 05	22.01±0.13	2.20±0.14	MG, IG	Same size and elong.
SA1656-007	12 59 49.0	27 57 20	21.71±0.13	2.53±0.14	DG	Sprial w/material arnd.
SA1656-008	12 59 49.5	27 55 30	18.66±0.02	2.16±0.02	AG	RB 55
SA1656-009	12 59 47.0	27 55 07	22.96±0.21	1.94±0.24	DG	LSB
SA1656-010	12 59 49.0	27 54 42	21.30±0.08	2.19±0.90	IG or DG?	
SA1656-011	12 59 57.0	27 55 55	19.12±0.03	1.72±0.04	IG	Sa and E, RB64
SA1656-012	13 00 02.0	27 56 40	20.30±0.03	1.72±0.03	IG	RB 71
SA1656-013	13 00 03.0	27 56 42	23.52±0.29	1.56±0.34	IG	LSB, one D.
SA1656-014	12 59 07.0	27 57 00	22.18±0.20	2.36±0.20	dwG	
SA1656-015	12 59 10.0	27 58 30	22.30±0.10	1.47±0.11	TG	
SA1656-016	12 59 17.5	27 57 15	21.17±0.05	1.78±0.05	TG	
SA1656-017	12 59 19.5	27 58 05	20.59±0.03	1.34±0.05	TG	Lrg. red tail
SA1656-018	12 59 24.0	27 53 55	20.55±0.03	1.43±0.03	DG	a bent S0 18 w/comp.
SA1656-019	12 59 23.0	27 54 42	17.23±0.01	1.94±0.01	dwG	cntrd on NGC4869
SA1656-020	12 59 23.0	27 57 05	22.90±0.17	1.56±0.20	DG	possible dwf irregular
SA1656-021	12 59 26.0	27 58 25	18.60±0.02	1.74±0.02	MG	RB 141
SA1656-022	12 59 21.0	27 57 25	22.28±0.10	1.55±0.12	TG	Slight Tail
SA1656-023	12 58 46.0	27 45 25	23.10±0.12	1.03±0.15	TG	Blue Tail
SA1656-024	12 58 47.0	27 44 25	20.70±0.04	2.19±0.04	IG	one b, one LSB
SA1656-025	12 58 51.0	27 44 15	24.22±0.32	1.07±0.42	DG	very faint

Table 6 Cont.: Structures in Coma Cluster

Name	R.A.(J2000)	Dec (J2000)	R	B-R	Morphology	Notes
SA1656-026	12 58 45.0	27 46 30	19.56±0.02	2.44±0.02	MG	
SA1656-027	12 58 49.0	27 47 25	22.63±0.10	1.31±0.12	MG, DG	3 gal, one wtail
SA1656-028	12 58 53.5	27 48 00	21.99±0.08	1.58±0.10	TG	large gal.
SA1656-029	12 58 55.0	27 50 11	21.56±0.05	1.50±0.06	DG	debris arc
SA1656-030	12 58 50.0	27 49 10	19.83±0.02	1.81±0.02	MG	
SA1656-031	12 58 54.0	27 49 30	22.30±0.10	1.66±0.11	LG	
SA1656-032	12 58 55.0	27 47 50	19.39±0.01	1.63±0.02	MG	RB 210
SA1656-033	12 59 00.0	27 46 05	18.89±0.03	2.23±0.03	DG	spiral
SA1656-034	12 58 56.1	27 47 10	21.94±0.06	1.48±0.08	TG	LG in R
SA1656-035	12 58 55.0	27 44 25	20.82±0.02	1.18±0.03	MG	3 gal.
SA1656-036	12 59 01.0	27 45 37	19.57±0.03	2.98±0.03	MG	4 galaxies
SA1656-037	12 59 03.0	27 47 00	22.77±0.14	1.53±0.16	MG	2 galaxies
SA1656-038	12 58 56.0	27 48 13	20.34±0.02	1.77±0.03	MG	One lrg. One sml.
SA1656-039	12 59 04.0	27 49 35	21.27±0.06	2.00±0.06	TG	object at tail's end
SA1656-040	12 59 02.5	27 49 30	22.75±0.08	0.82±0.11	LG	Near another gal.
SA1656-041	12 59 04.5	27 47 40	21.70±0.03	0.76±0.03	TG	
SA1656-042	12 59 05.0	27 47 55	19.89±0.03	2.56±0.03	MG	One LSB
SA1656-043	12 59 15.0	27 46 15	20.40±0.06	2.99±0.07	MG	
SA1656-044	12 59 06.5	27 44 45	22.33±0.15	2.03±0.16	IG	DG in B
SA1656-045	12 59 09.0	27 44 30	21.93±0.07	1.67±0.08	MG	Very close
SA1656-046	12 59 12.0	27 47 05	22.28±0.12	1.90±0.13	TG	LG in R
SA1656-047	12 59 12.0	27 49 55	22.55±0.13	1.78±0.14	MG	faint and close
SA1656-048	12 58 47.5	27 49 50	22.55±0.16	2.00±0.18	TG	not vis. in B
SA1656-049	12 58 55.0	27 49 35	19.99±0.03	2.38±0.03	TG	large S0
SA1656-050	12 59 06.0	27 46 10	22.51±0.28	2.65±0.29	LG	

Table 6 Cont.: Structures in Coma Cluster

Name	R.A.(J2000)	Dec (J2000)	R	B-R	Morphology	Notes
SA1656-051	12 58 51.0	27 46 45	16.48±0.01	0.60±0.01	MG	
SA1656-052	12 59 14.0	27 46 30	17.43±0.01	2.17±0.02	DG	Large E with Shells
SA1656-053	12 59 10.0	27 47 10	21.37±0.03	1.18±0.03	TG	
SA1656-054	12 59 51.0	27 50 00	19.39±0.05	1.88±0.07	AG	RB 60
SA1656-055	12 59 46.0	27 51 30	17.69±0.03	2.64±0.04	AG?	RB 49
SA1656-056	12 59 47.5	27 49 37	22.49±0.11	1.33±0.14	TG	
SA1656-057	12 59 44.2	27 54 35	23.48±0.24	1.18±0.30	TG	NGC 4876
SA1656-058	12 59 50.0	27 54 30	21.09±0.06	1.50±0.08	MG, IG	one mem. a disk system
SA1656-059	12 59 51.0	27 52 17	22.99±0.28	1.89±0.30	MG	f pair
SA1656-060	12 59 52.5	27 49 25	21.50±0.06	1.55±0.08	TG	pos. dwf companion
SA1656-061	12 59 58.5	27 51 57	23.11±0.19	1.17±0.24	MG, IG	
SA1656-062	13 00 07.0	27 52 49	22.11±0.14	1.946±0.15	LG	pos. sprl/edge on, bent arr
SA1656-063	13 00 07.7	27 51 30	23.16±0.27	1.70±0.31	DG	
SA1656-064	13 00 09.0	27 51 57	19.26±0.05	0.93±0.08	IG	diffuse debris nearby
SA1656-065	13 00 06.0	27 48 35	23.64±0.32	1.34±0.27	IG	CGCG 160-240
SA1656-066	13 00 06.0	28 01 30	19.69±0.04	1.20±0.07	AG?	RB 74
SA1656-067	13 00 04.0	28 03 00	23.34±0.17	1.04±0.21	dwG, IG	
SA1656-068	13 00 04.0	28 03 40	23.36±0.30	1.70±0.34	MG	3 gal
SA1656-069	13 00 12.5	28 04 30	18.03±0.03	1.73±0.04	AG	RB 87
SA1656-070	13 00 13.0	28 05 20	21.55±0.17	2.23±0.20	DG	slight
SA1656-071	13 00 13.0	28 03 15	21.23±0.06	1.11±0.10	LG	very flat, and bent
SA1656-072	13 00 22.0	28 02 30	22.59±0.07	0.74±0.10	TG	
SA1656-073	13 00 26.5	28 04 00	21.15±0.10	2.87±0.11	LG	possible tail in R
SA1656-074	13 00 29.0	28 05 25	23.31±0.26	1.73±0.30	MG	
SA1656-075	13 00 27.0	28 04 30	22.75±0.12	1.25±0.14	IG	two tails joining

Table 6 Cont.: Structures in Coma Cluster

Name	R.A.(J2000)	Dec (J2000)	R	B-R	Morphology	Notes
SA1656-076	13 00 27.5	28 04 15	22.07±0.15	2.13±0.17	MG	4 gal
SA1656-077	13 00 26.0	28 03 55	22.29±0.08	1.17±0.11	dwG	main gal. w/tail
SA1656-078	13 00 27.0	28 01 20	23.12±0.34	2.06±0.40	TG, MG	possible arc
SA1656-079	12 58 38.0	28 08 05	17.32±0.01	2.27±0.01	dwG, MG	
SA1656-080	12 58 39.5	28 09 55	21.80±0.18	2.75±0.19	TG	
SA1656-081	12 58 42.0	28 11 05	21.17±0.10	1.97±0.12	AG	LSB material, debris
SA1656-082	12 58 46.0	28 06 25	22.23±0.19	2.43±0.20	MG	DG in B
SA1656-083	12 58 48.0	28 05 30	20.55±0.10	3.51±0.11	TG	knots in R
SA1656-084	12 58 59.0	28 07 05	23.59±0.40	1.73±0.44	DG	very distored, two red knot
SA1656-085	12 59 02.0	28 07 00	19.87±0.09	1.60±0.12	AG, MG	N4858 & N4860
SA1656-086	12 58 59.0	28 09 45	22.83±0.24	2.11±0.26	LG	Tailed in R
SA1656-087	12 59 02.0	28 09 55	19.96±0.05	2.91±0.05	MG	triple, l cntr
SA1656-088	12 58 46.0	28 10 10	21.84±0.38	3.66±0.40	TG	2 red knots
SA1656-089	12 59 52.3	28 12 20	21.80±0.05	0.87±0.06	TG	
SA1656-090	12 59 47.0	28 16 25	19.96±0.04	1.89±0.04	AG?	mat. arnd gal. w/bridge
SA1656-091	12 59 55.5	28 16 50	21.25±0.08	1.95±0.09	TG	
SA1656-092	12 59 51.0	28 17 45	20.92±0.03	0.78±0.04	AG	
SA1656-093	13 00 03.0	28 13 05	17.20±0.01	2.75±0.02	MG	3 members
SA1656-094	13 00 02.5	28 12 55	23.27±0.21	1.14±0.26	TG	not obvious in R
SA1656-095	13 00 06.0	28 15 05	24.58±0.36	-0.17±0.95	DG	lrg
SA1656-096	13 00 08.0	28 13 35	23.41±0.43	1.76±0.48	DG	
SA1656-097	13 00 12.0	28 12 45	22.17±0.08	1.07±0.09	TG	
SA1656-098	13 00 12.0	28 11 30	23.25±0.30	1.48±0.32	TG	f
SA1656-099	13 00 01.0	28 15 05	22.12±0.04	-0.01±0.08	TG	Blue Tail
SA1656-100	12 59 59.0	28 14 05	20.78±0.32	3.96±0.34	LG	Large

Table 6 Cont.: Structures in Coma Cluster

Name	R.A.(J2000)	Dec (J2000)	R	B-R	Morphology	Notes
SA1656-101	13 00 04.0	28 15 35	21.97±0.15	1.70±0.20	TG	Curved Tail
SA1656-102	13 00 43.0	27 58 05	17.82±0.05	2.31±0.07	MG	RB113 & IC4042
SA1656-103	13 00 43.0	27 58 15	17.82±0.05	2.31±0.07	DG	SA0/a w/shells
SA1656-104	13 00 46.5	27 59 50	21.65±0.17	2.04±0.18	MG	s and l, blends in B
SA1656-105	13 00 43.0	28 03 25	22.32±0.17	1.53±0.20	dwG	line of galaxies
SA1656-106	13 00 51.0	28 02 45	18.84±0.09	0.76±0.11	MG	N4908
SA1656-107	13 00 52.5	27 59 57	24.04±0.56	1.22±0.64	TG	debris srndg
SA1656-108	13 00 53.0	27 58 10	21.520±0.10	1.33±0.13	MG	
SA1656-109	13 00 55.5	27 58 05	22.97±0.32	1.69±0.35	MG	s
SA1656-110	13 01 01.0	27 59 55	22.70±0.43	2.37±0.46	MG	4 gal. in arc
SA1656-111	13 01 02.0	28 00 40	23.44±1.20	2.75±1.30	TG	
SA1656-112	13 01 05.0	28 03 50	20.49±0.06	1.43±0.08	AG	
SA1656-113	13 01 05.0	28 03 35	23.78±0.42	1.31±0.50	DG	bits of material
SA1656-114	13 01 05.0	28 01 30	19.12±0.02	1.34±0.02	MG	
SA1656-115	13 01 03.5	27 59 55	21.51±0.06	1.17±0.08	MG	
SA1656-116	13 01 05.0	27 58 20	21.19±0.08	1.76±0.09	MG	s, l

Table 7: Structures Found in Perseus Cluster (Abell 0426)

Name	R.A.(J2000)	Dec (J2000)	Morphology	Notes
SA0426-01	03 19 48.0	41 30 45	DG	Perseus A
SA0426-02	03 19 40.0	41 31 00	DG	butterfly Shaped
SA0426-03	03 19 45.3	41 33 36	TG	
SA0426-04	03 19 40.2	41 33 55	TG	
SA0426-05	03 19 42.0	41 34 30	MG	Sprls
SA0426-06	03 19 43.5	41 34 35	TG	
SA0426-07	03 19 39.5	41 35 50	DG	twisted Gal
SA0426-08	03 19 48.0	41 35 05	TG	
SA0426-09	03 19 44.0	41 35 30	TG	s
SA0426-10	03 19 57.6	41 36 00	DG or MG	im peanut Shp
SA0426-11	03 19 51.0	41 34 18	DG	flat btm
SA0426-12	03 19 56.8	41 32 50	DG	a LSB Sprl
SA0426-13	03 20 06.0	41 31 10	MG, LG	
SA0426-14	03 20 12.8	41 30 55	DG	LSB
SA0426-15	03 20 03.5	41 30 35	DG	diffuse
SA0426-16	03 20 08.5	41 31 10	DG	Peanut Shp
SA0426-17	03 20 10.0	41 30 25	IG	sprl
SA0426-18	03 20 05.0	41 32 03	DG, TG	very disturbed
SA0426-19	03 20 03.0	41 31 45	DG, TG	extented halo mat.
SA0426-20	03 20 10.5	41 32 00	TG	
SA0426-21	03 20 05.0	41 31 07	MG	
SA0426-22	03 20 07.0	41 35 00	TG	
SA0426-23	03 20 00.5	41 35 10	DG	batman Galaxy
SA0426-24	03 20 11.5	41 35 15	DG	looks blown up
SA0426-25	03 20 02.0	41 31 10	IG	faint bridge

Table 7 Cont.: Structures in Perseus Cluster

Name	R.A.(J2000)	Dec (J2000)	Morphology	Notes
SA0426-26	03 19 33.0	41 26 15	LG	
SA0426-27	03 19 36.5	41 26 25	MG, IG	
SA0426-28	03 19 41.0	41 26 00	MG or DG	
SA0426-29	03 19 38.0	41 25 57	LG	near an E
SA0426-30	03 19 43.5	41 28 55	LG	very flat
SA0426-31	03 19 41.0	41 29 25	LG	
SA0426-32	03 19 33.0	41 28 35	TG	
SA0426-33	03 19 37.5	41 29 25	DG	LSB
SA0426-34	03 19 34.0	41 29 23	MG or DG	
SA0426-35	03 19 35.0	41 28 13	IG	smudgy
SA0426-36	03 19 33.0	41 30 55	DG	
SA0426-37	03 19 39.5	41 30 30	DG	
SA0426-38	03 19 38.0	41 29 57	TG, LG	
SA0426-39	03 19 32.0	41 30 20	dwG	
SA0426-40	03 19 36.0	41 31 50	DG	LSB
SA0426-41	03 19 51.5	41 31 25	TG	thick
SA0426-42	03 19 46.0	41 30 05	LG	
SA0426-43	03 19 50.0	41 29 52	DG	smuge
SA0426-44	03 19 46.5	41 29 05	LG	
SA0426-45	03 19 46.0	41 28 55	IG, dwG	bits of material
SAO426-46	03 19 47.0	41 28 50	DG	LSB
SA0426-47	03 19 45.0	41 28 07	DG	smuge
SA0426-48	03 19 48.5	41 27 30	MG	
SA0426-49	03 19 50.0	41 26 50	LG	LSB
SA0426-50	03 19 51.0	41 26 10	IG	box Like

Table 7 Cont.: Structures in Perseus Cluster

Name	R.A.(J2000)	Dec (J2000)	Morphology	Notes
SA0426-51	03 19 46.0	41 26 12	MG	
SA0426-52	03 19 49.0	41 25 35	DG	smudge
SA0426-53	03 19 53.5	41 25 45	DG	boxy, smudge, LSB
SA0426-54	03 19 58.0	41 25 45	DG	ring Gal.
SA0426-55	03 20 04.5	41 25 45	DG	LSB
SA0426-56	03 20 04.0	41 26 55	TG	
SA0426-57	03 20 03.5	41 27 55	LG	
SA0426-58	03 20 05.0	41 27 35	TG	bent
SA0426-59	03 20 06.0	41 29 00	LG	
SA0426-60	03 20 57.0	41 29 25	DG	smudge
SA0426-61	03 20 00.5	41 30 00	LG	flattened
SA0426-62	03 20 05.0	41 31 07	MG	
SA0426-63	03 20 00.3	41 30 45	TG	
SA0426-64	03 20 03.0	41 31 05	LG	bright core/halo
SA0426-65	03 20 03.5	41 30 30	DG	
SA0426-66	03 20 02.0	41 30 03	DG	diffuse
SA0426-67	03 20 04.0	41 31 30	DG	
SA0426-68	03 20 05.5	41 30 45	LG	
SA0426-69	03 20 03.5	41 03 20	DG	boxy

Table 8: Structures Found in Abell 2199

Name	R.A.(J2000)	Dec (J2000)	R	(B-R)	Morphology	Notes
SA2199-01	16 28 26.0	39 28 30	16.90±0.01	1.45±0.01	TG	slight
SA2199-02	16 28 23.0	39 29 40	22.18±0.10	1.65±0.11	MG	
SA2199-03	16 28 30.0	39 30 30	21.66±0.11	2.30±0.12	MG	
SA2199-04	16 28 22.0	39 31 10	20.89±0.07	2.65±0.08	dwG	
SA2199-05	16 28 26.0	39 29 40	21.68±0.27	3.40±0.28	dwG	
SA2199-06	16 28 24.5	39 33 30	16.30±0.01	1.26±0.01	MG	
SA2199-07	16 28 27.0	39 32 45	16.93±0.01	1.41±0.02	MG	s comp
SA2199-08	16 28 26.5	39 33 15	21.96±0.16	2.35±0.17	DG	
SA2199-09	16 28 30.0	39 34 00	24.01±0.54	1.79±0.60	LG	
SA2199-10	16 28 38.0	39 33 00	20.95±0.18	0.73±0.41	DG	NGC 6166
SA2199-11	16 28 31.0	39 31 10	17.03±0.02	1.96±0.03	MG	
SA2199-12	16 28 40.5	39 29 55	21.56±0.11	2.52±0.12	MG	ringed
SA2199-13	16 28 36.0	39 30 25	23.41±0.24	1.55±0.28	DG	
SA2199-14	16 28 37.0	39 29 10	21.72±0.12	1.99±0.14	TG	
SA2199-15	16 28 35.0	39 28 40	21.87±0.08	1.86±0.09	TG	
SA2199-16	16 28 37.0	39 28 50	23.04±0.03	-1.02±0.08	TG	
SA2199-17	16 28 45.0	39 28 35	20.01±0.07	1.83±0.09	DG	with arm
SA2199-18	16 28 45.0	39 29 05	17.87±0.02	2.24±0.03	MG	sprl
SA2199-19	16 28 44.0	39 28 00	20.67±0.08	2.41±0.10	DG	
SA2199-20	16 28 48.5	39 30 55	20.58±0.05	2.42±0.05	TG?	
SA2199-21	16 28 47.0	39 31 10	22.41±0.16	2.11±0.17	DG	
SA2199-22	16 28 48.0	39 31 35	22.41±0.14	1.86±0.16	MG	
SA2199-23	16 28 49.5	39 34 10	19.07±0.02	1.61±0.02	MG	
SA2199-24	16 28 43.0	39 34 05	21.28±0.15	3.27±0.15	TG	
SA2199-25	16 28 49.0	39 32 50	17.20±0.01	0.24±0.01	DG	

Table 8 Cont.: Structures in Cluster Abell 2199

Name	R.A.(J2000)	Dec (J2000)	R	(B-R)	Morphology	Notes
SA2199-26	16 28 54.0	39 31 35	20.27±0.07	3.25±0.07	DG	
SA2199-27	16 28 53.0	39 32 45	23.36±0.48	2.49±0.51	TG	
SA2199-28	16 28 53.0	39 29 00	16.60±0.01	1.47±0.02	TG, IG	
SA2199-29	16 28 50.5	39 29 30	22.27±0.36	3.22±0.37	TG	
SA2199-30	16 28 50.5	39 29 00	21.75±0.03	0.51±0.04	MG	

Table 9: Structures Found in Cluster AWM 5

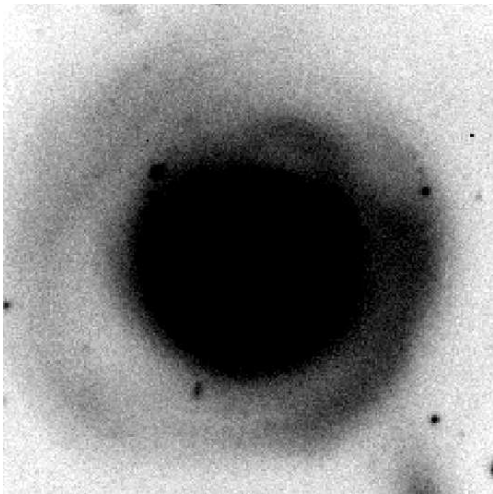
Name	R.A.(J2000)	Dec (J2000)	R	(B-R)	Morphology	Notes
SAWM5-01	16 57 48.0	27 48 00	16.03±0.01	0.50±0.02	IG	one a disk gal.
SAWM5-02	16 57 46.5	27 48 50	20.82±0.05	2.33±0.05	MG	a LSB and HSB Es
SAWM5-03	16 57 44.1	27 49 33	18.85±0.01	1.49±0.02	MG	l and s
SAWM5-04	16 57 45.0	27 50 45	18.24±0.02	3.36±0.02	MG	equal b
SAWM5-05	16 57 49.0	27 51 22	22.25±0.09	1.45±0.11	LG	one end larger
SAWM5-06	16 57 48.5	27 51 32	16.82±0.01	1.44±0.02	MG	f and b
SAWM5-07	16 57 49.5	27 51 40	21.66±0.11	2.03±0.12	LG	
SAWM5-08	16 57 53.0	27 53 07	21.17±0.05	1.89±0.06	MG	
SAWM5-09	16 57 55.0	27 52 10	17.79±0.02	1.98±0.02	IG	large galaxies
SAWM5-10	16 57 58.0	27 51 50	23.24±0.50	2.65±0.60	TG	
SAWM5-11	16 57 55.0	27 51 05	21.37±0.10	2.14±0.11	DG	bubble shaped
SAWM5-12	16 58 00.2	27 48 20	20.94±0.05	1.93±0.06	IG	
SAWM5-13	16 58 06.5	27 48 40	19.50±0.02	1.50±0.02	MG	3 gal. w/similar b.
SAWM5-14	16 58 03.5	27 49 30	23.21±0.11	0.80±0.18	LG	two LSB thin lines
SAWM5-15	16 58 01.0	27 48 30	22.47±0.12	1.44±0.15	MG	faint
SAWM5-16	16 58 03.0	27 50 10	19.66±0.02	1.54±0.02	MG	
SAWM5-17	16 58 10.0	27 50 25	20.13±0.04	1.73±0.06	AG?	knots distant
SAWM5-18	16 58 01.5	27 52 32	16.37±0.01	0.89±0.01	DG	s. gal. nearby
SAWM5-19	16 58 00.2	27 53 25	18.26±0.02	1.94±0.02	TG	near another gal.
SAWM5-20	16 58 12.0	27 53 50	19.70±0.04	3.08±0.04	MG	
SAWM5-21	16 58 06.0	27 51 25	22.40±0.03	-0.96±0.06	TG	near another gal., peanut sh
SAWM5-22	16 58 05.0	27 48 55	24.11±0.50	1.56±0.60	TG	
SAWM5-23	16 58 10.5	27 48 25	16.17±0.01	2.04±0.01	MG	l. gal. w/two comp.

Table 10: Structures Found in Cluster AWM 3

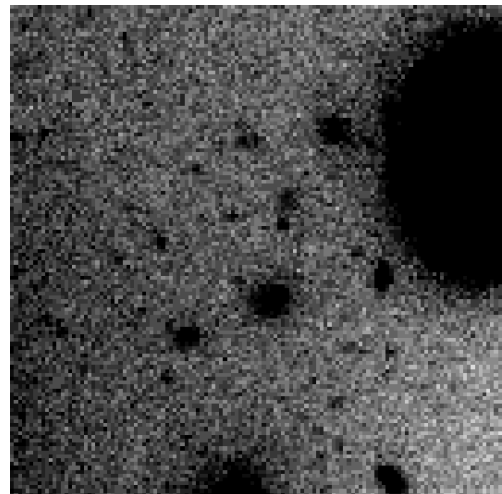
Name	R.A.(J2000)	Dec (J2000)	Morphology	Notes
SAWM3-01	14 28 04.0	25 48 50	DG	LSB
SAWM3-02	14 27 57.0	25 47 45	TG	
SAWM3-03	14 27 56.0	25 47 50	TG	
SAWM3-04	14 28 00.0	25 51 50	DG	slt halo
SAWM3-05	14 28 00.5	25 51 50	DG	
SAWM3-06	14 27 57.0	25 53 40	TG	
SAWM3-07	14 28 05.0	25 49 50	MG	
SAWM3-08	14 28 10.0	25 50 30	DG	twisted
SAWM3-09	14 28 07.0	25 49 05	TG	faint
SAWM3-10	14 28 11.0	25 50 55	DG	has shells, cD NGC 5629

Table 11: Objects identified with Redshifts

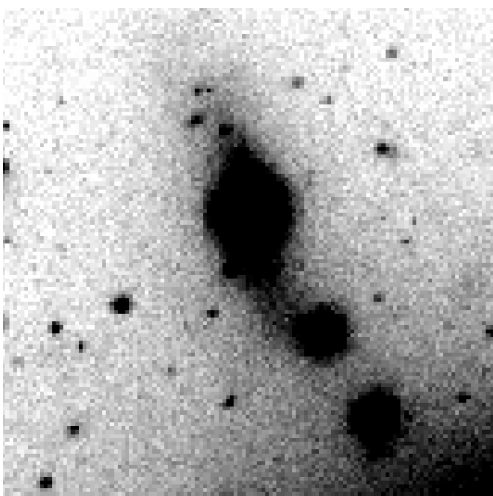
ID	R	B-R	morph	cz	Cluster _{cz}	$\delta(cz)$
SA1656-008	18.66±0.02	2.16±0.02	AG	9833	6917	2,916
SA1656-011	20.30±0.03	1.72±0.03	IG	7904	6917	987
SA1656-018	20.55±0.03	1.43±0.03	DG	18300	6917	11383
SA1656-019	17.23±0.01	1.94±0.01	dwG	6788	6917	-129
SA1656-026	19.56±0.02	2.44±0.02	MG	48108	6917	41191
SA1656-030	19.83±0.02	1.81±0.02	MG	35268	6917	28351
SA1656-032	19.39±0.01	1.63±0.02	MG	6448	6917	-469
SA1656-038	20.34±0.02	1.77±0.03	MG	7864	6917	947
SA1656-055	17.69±0.03	2.64±0.04	AG	8009	6917	1092
SA1656-057	23.48±0.24	1.18±0.30	TG	6629	6917	-288
SA1656-064	19.26±0.05	0.93±0.08	IG	5128	6917	-1789
SA1656-065	23.64±0.32	1.34±0.27	IG	6568	6917	-349
SA1656-066	19.69±0.04	1.20±0.07	AG?	5922	6917	-995
SA1656-069	18.03±0.03	1.73±0.04	AG	7493	6917	576
SA1656-071	21.23±0.06	1.11±0.10	LG	8135	6917	1218
SA1656-085	19.87±0.09	1.60±0.12	AG, MG	9436	6917	2519
SA1656-095	24.58±0.36	-0.17±0.95	DG	7569	6917	652
SA1656-103	17.82±0.05	2.31±0.07	MG	8366	6917	1449
SA1656-104	21.65±0.17	2.04±0.18	DG	6363	6917	-554
SA1656-106	18.84±0.09	0.76±0.11	MG	8784	6917	1867
SA1656-112	20.49±0.06	1.43±0.08	AG	2289	6917	-4628
SA0426-011	—	—	DG	4982	5486	-504
SA2199-010	20.95±0.18	0.73±0.41	DG	9324	9063	261
SA2199-011	17.03±0.02	1.96±0.03	MG	8957	9063	-106
SA2199-017	20.01±0.07	1.83±0.09	DG	8156	9063	-907
SA2199-018	17.87±0.02	2.24±0.03	MG	10163	9063	1100
SAWM3-010	—	—	DG	4489	4497	-8



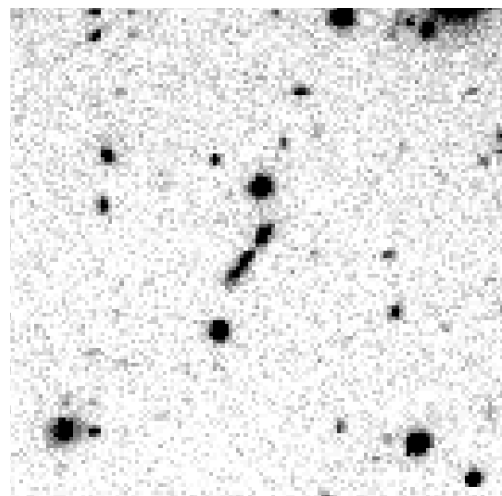
Distorted Galaxy (DG)



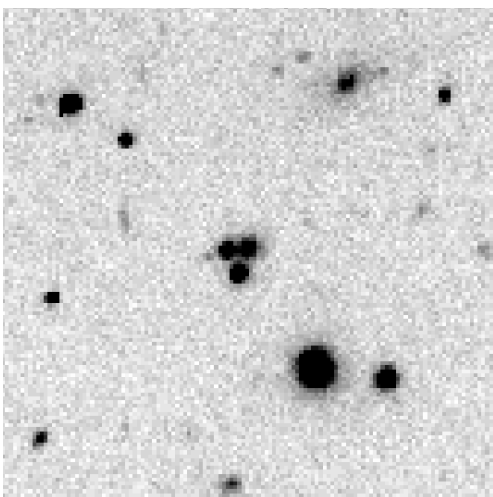
Dwarf Group (dwG)



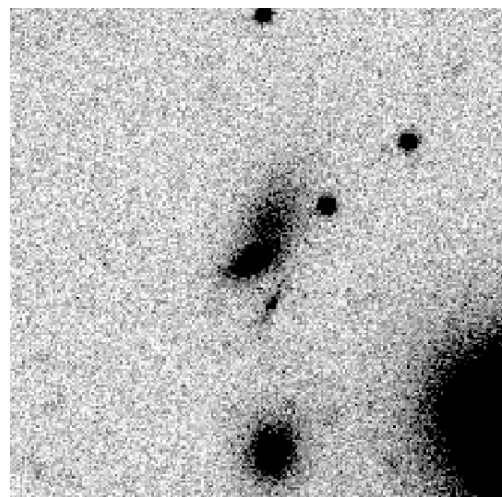
Interacting Galaxies (IG)



Line Galaxy (LG)



Multiple Galaxies (MG)



Tailed Galaxies (TG)

Fig. 1

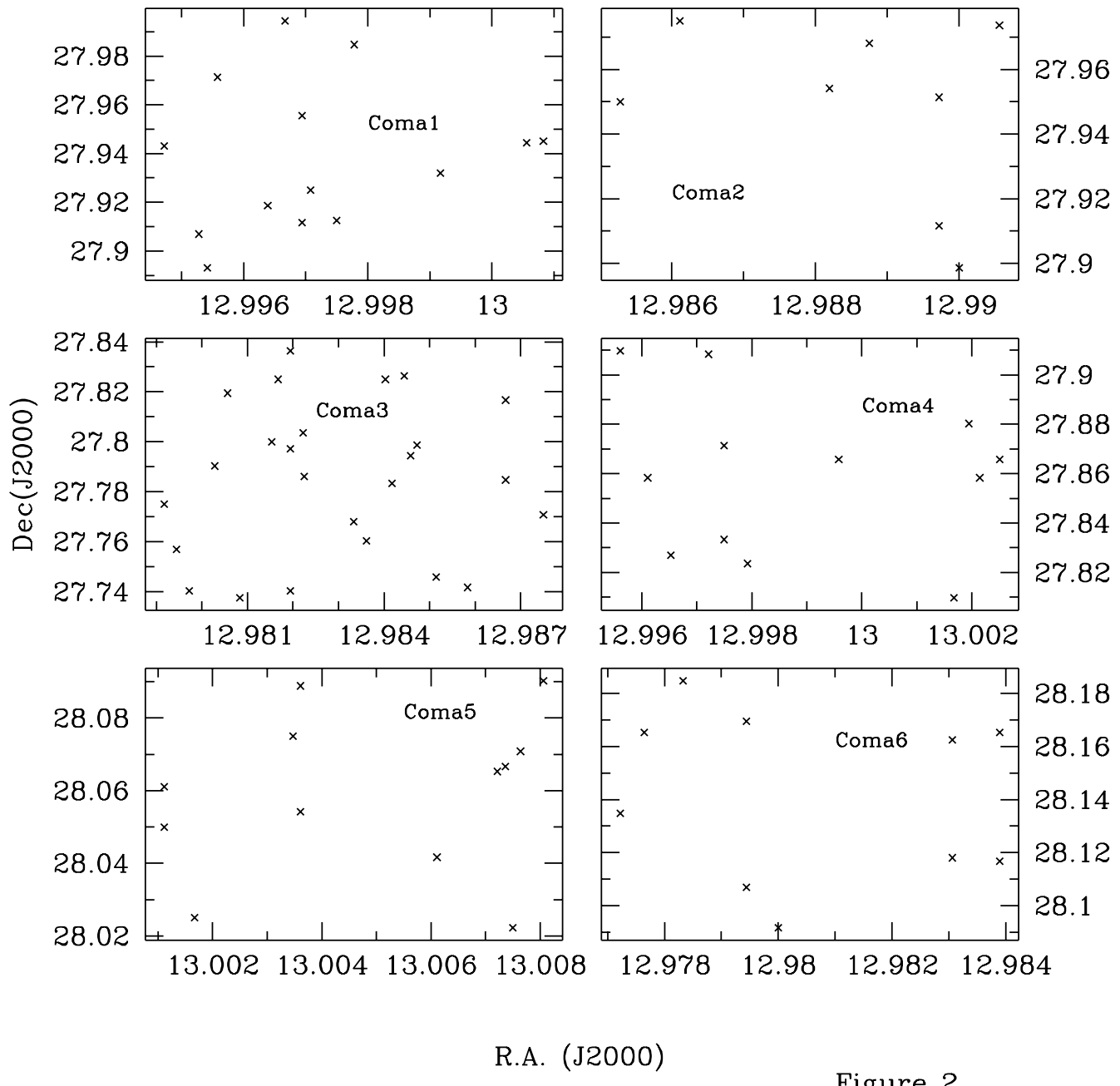


Figure 2

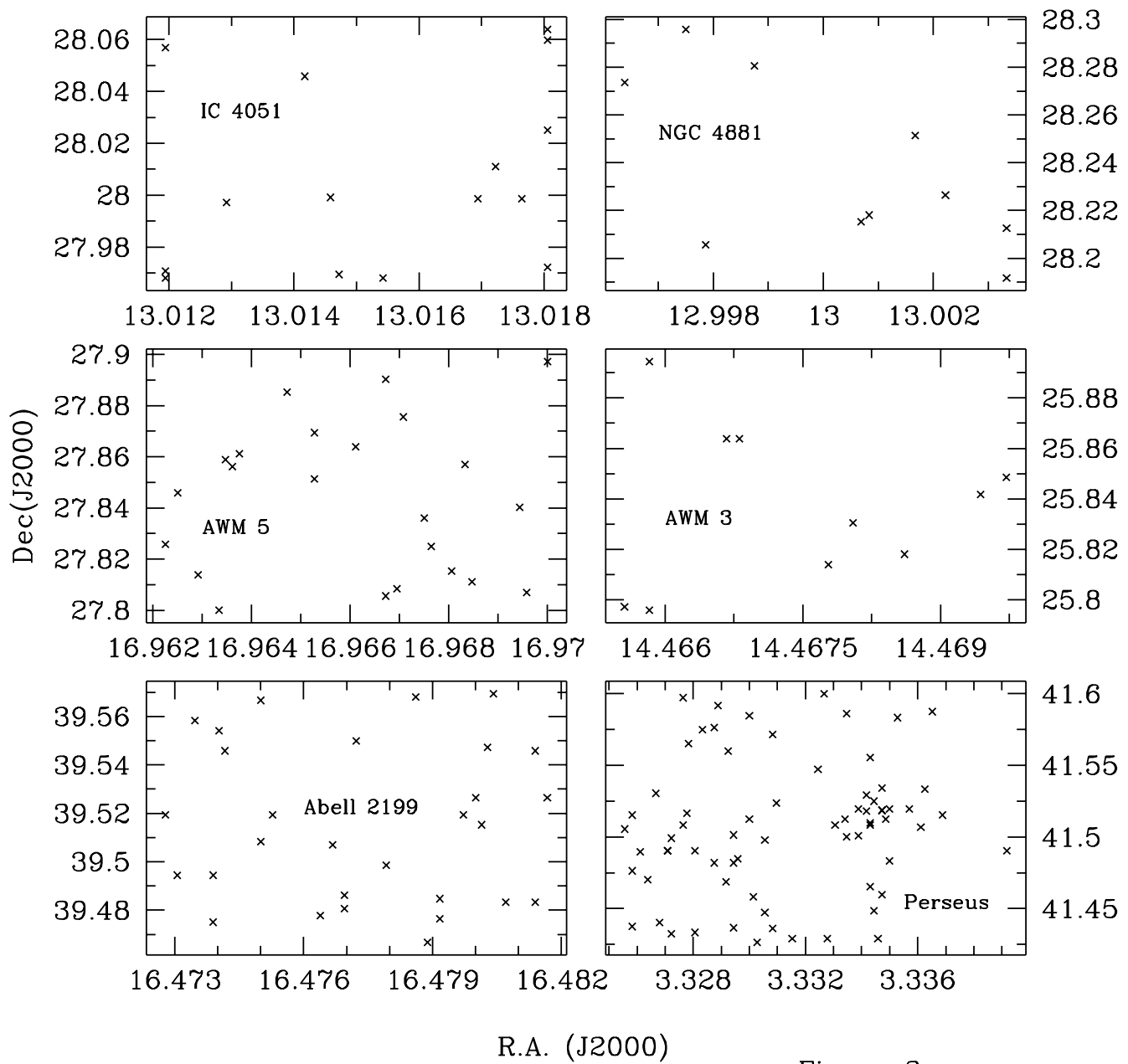


Figure 3

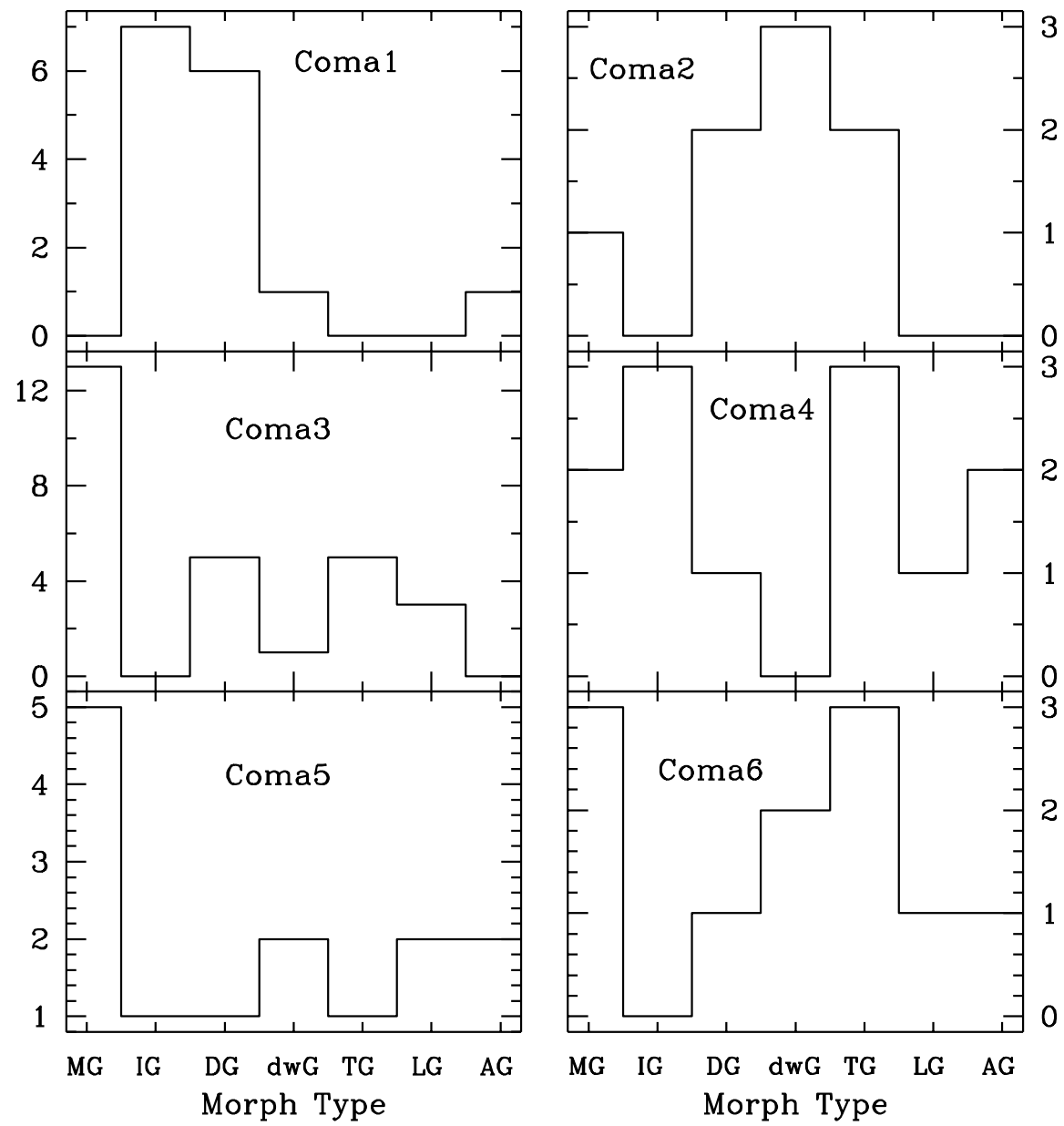


Figure 4

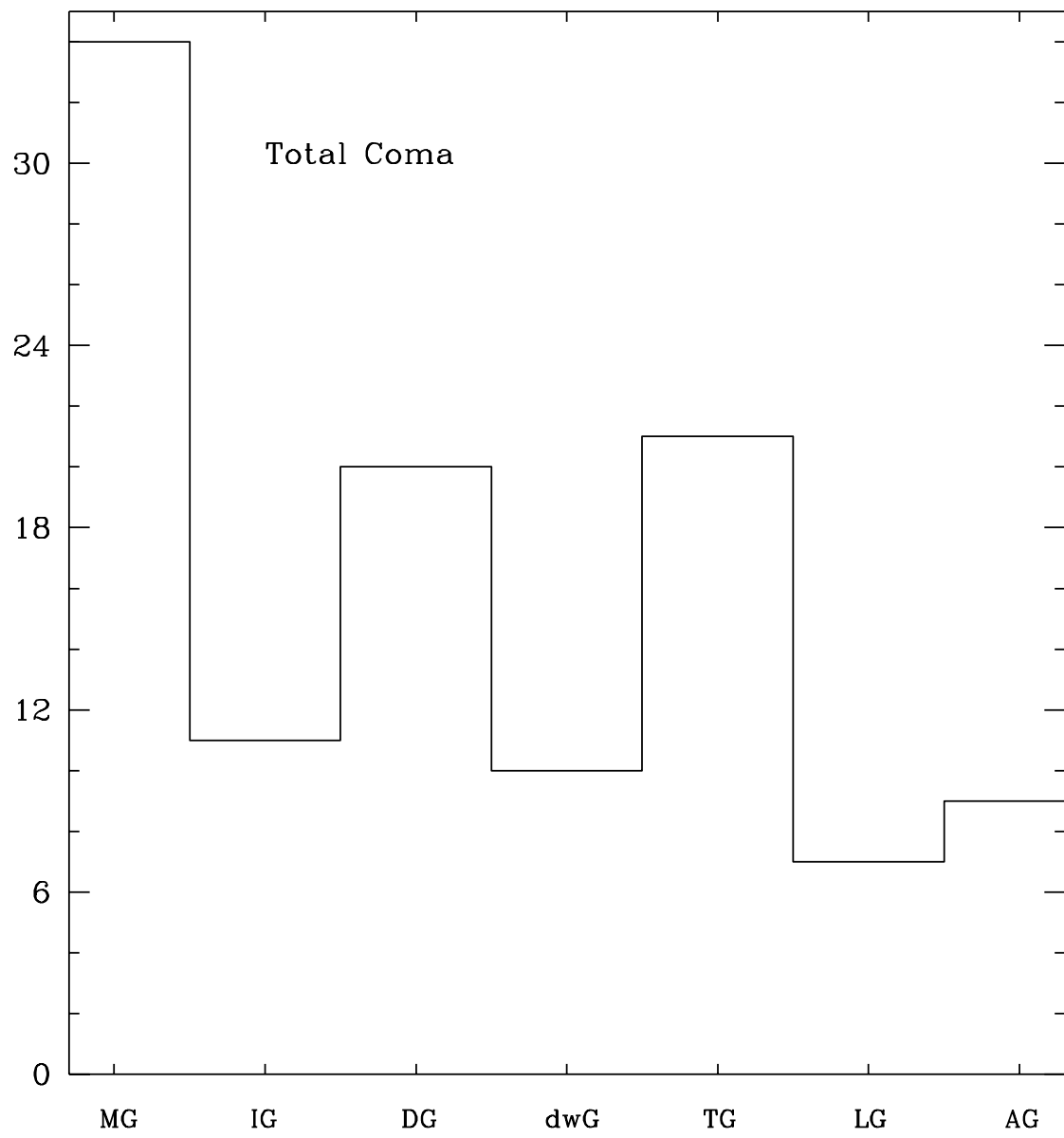


Figure 5

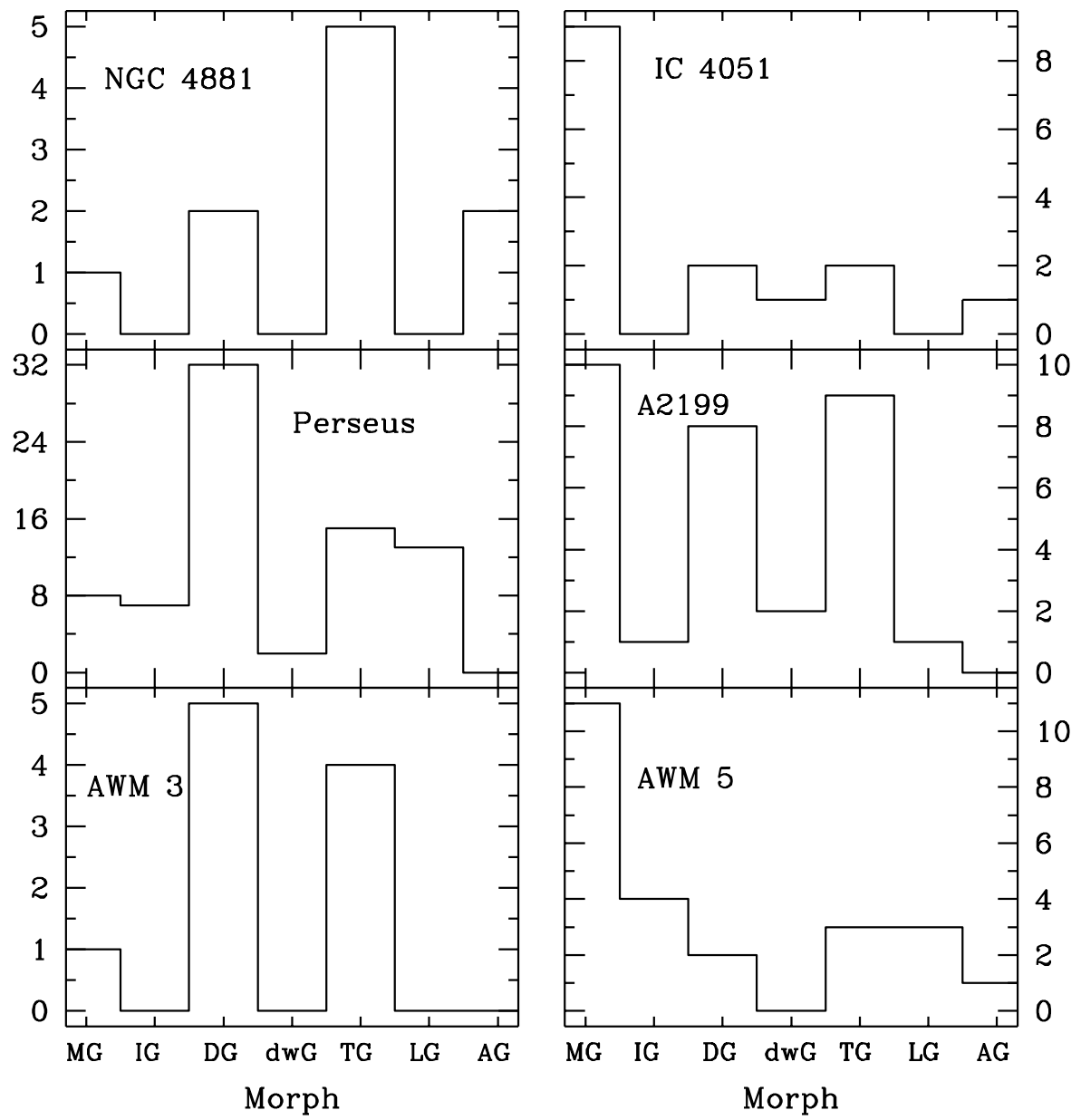


Figure 6

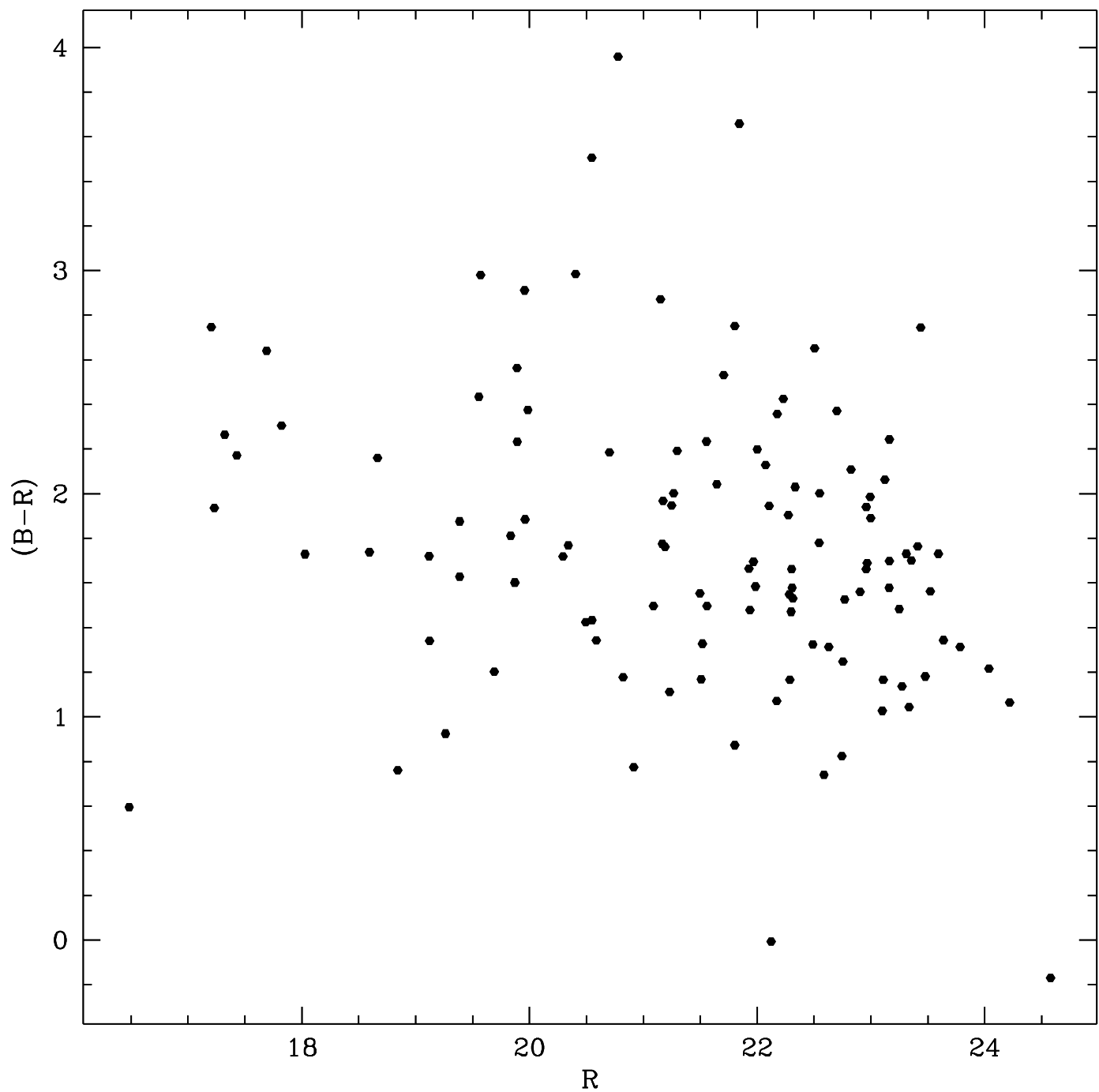


Figure 7

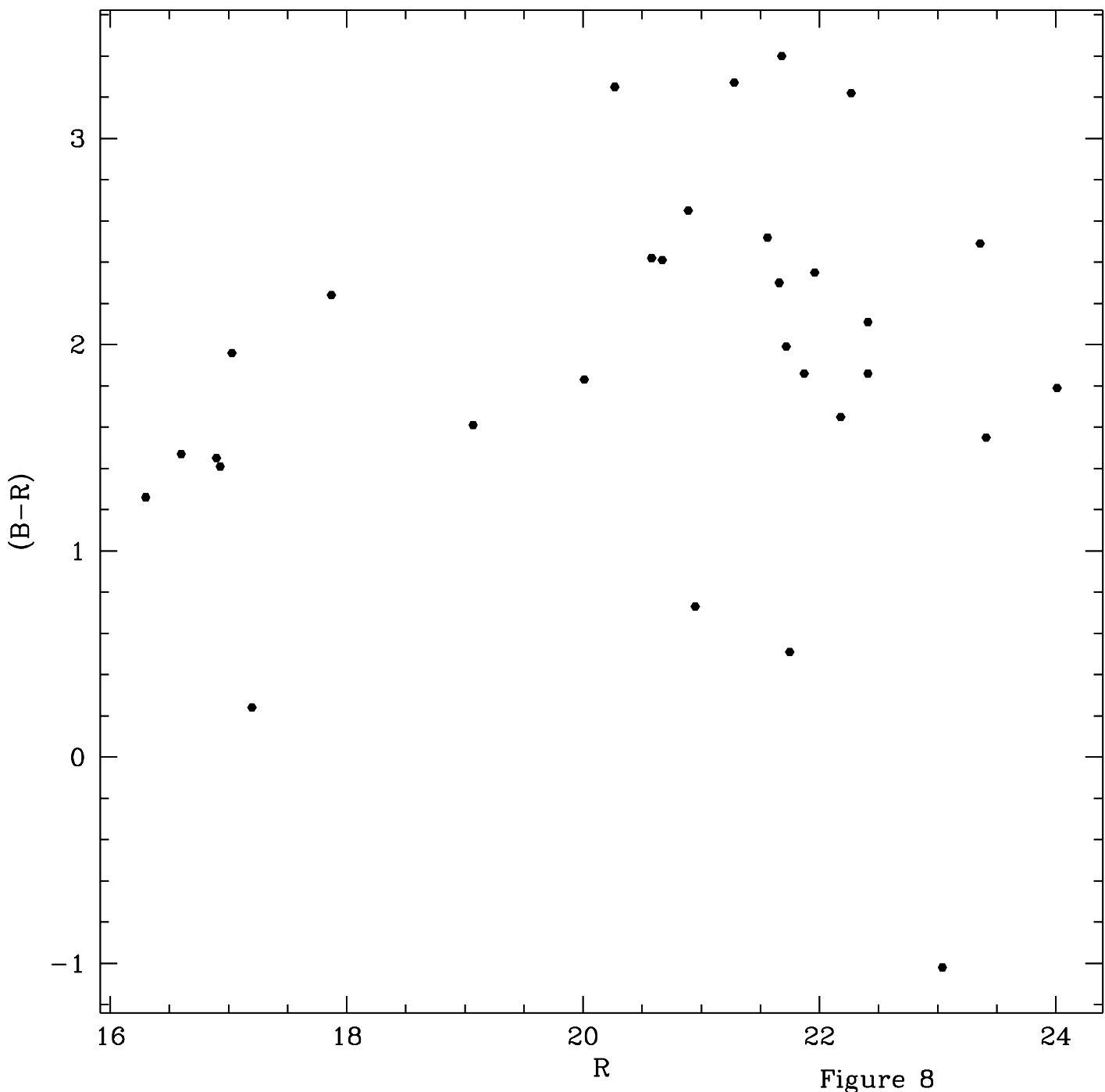


Figure 8

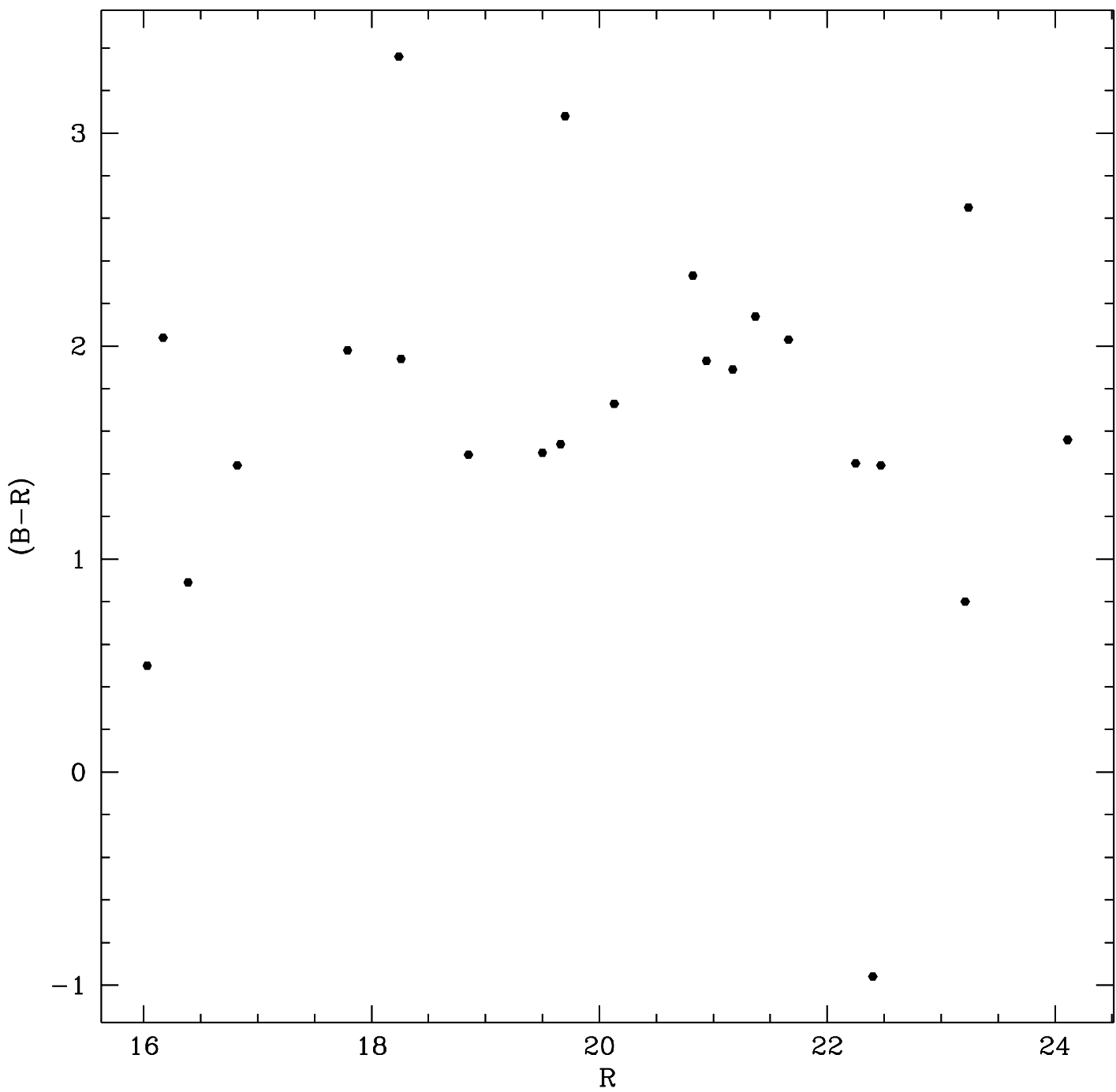


Figure 9

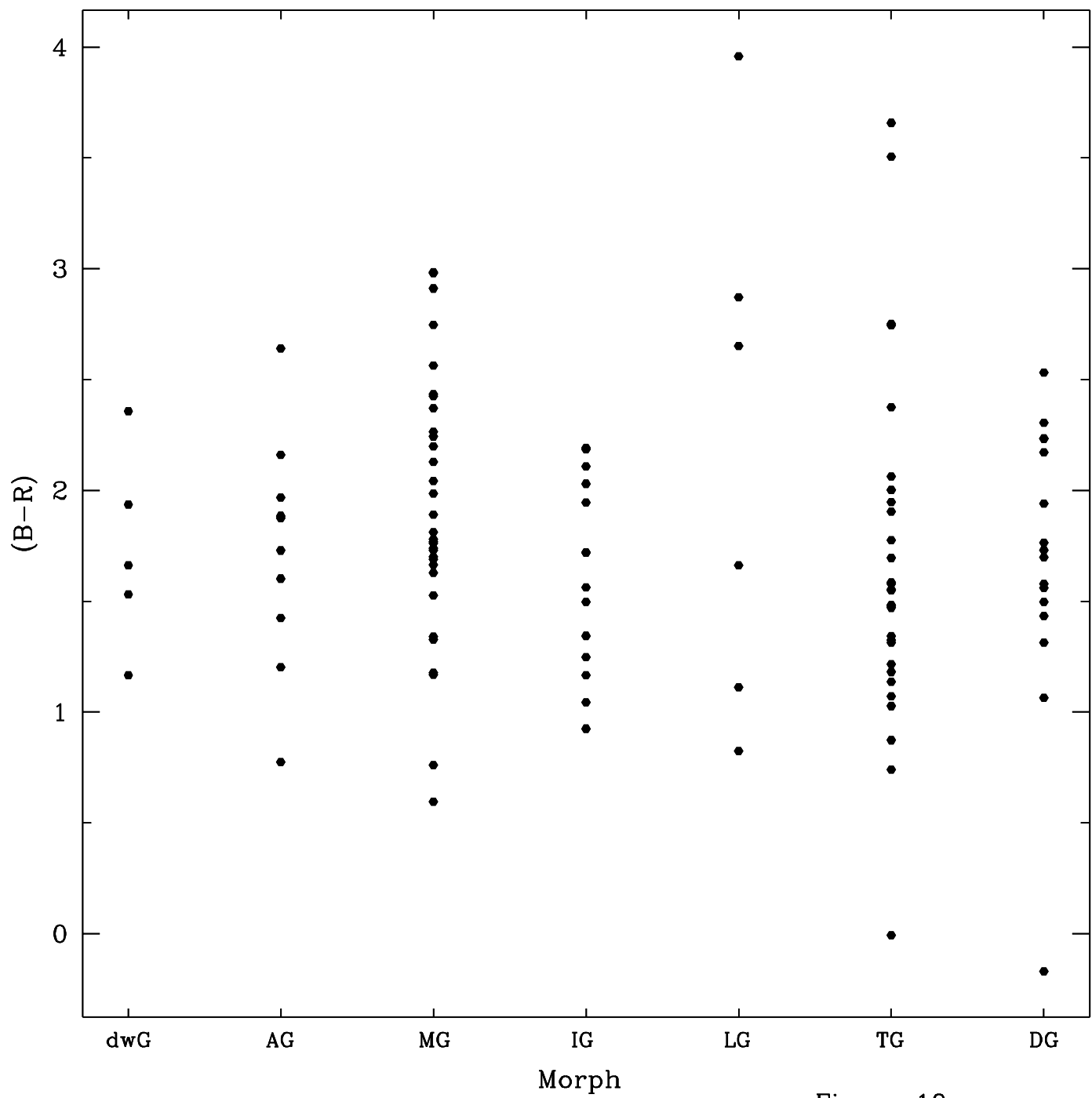


Figure 10

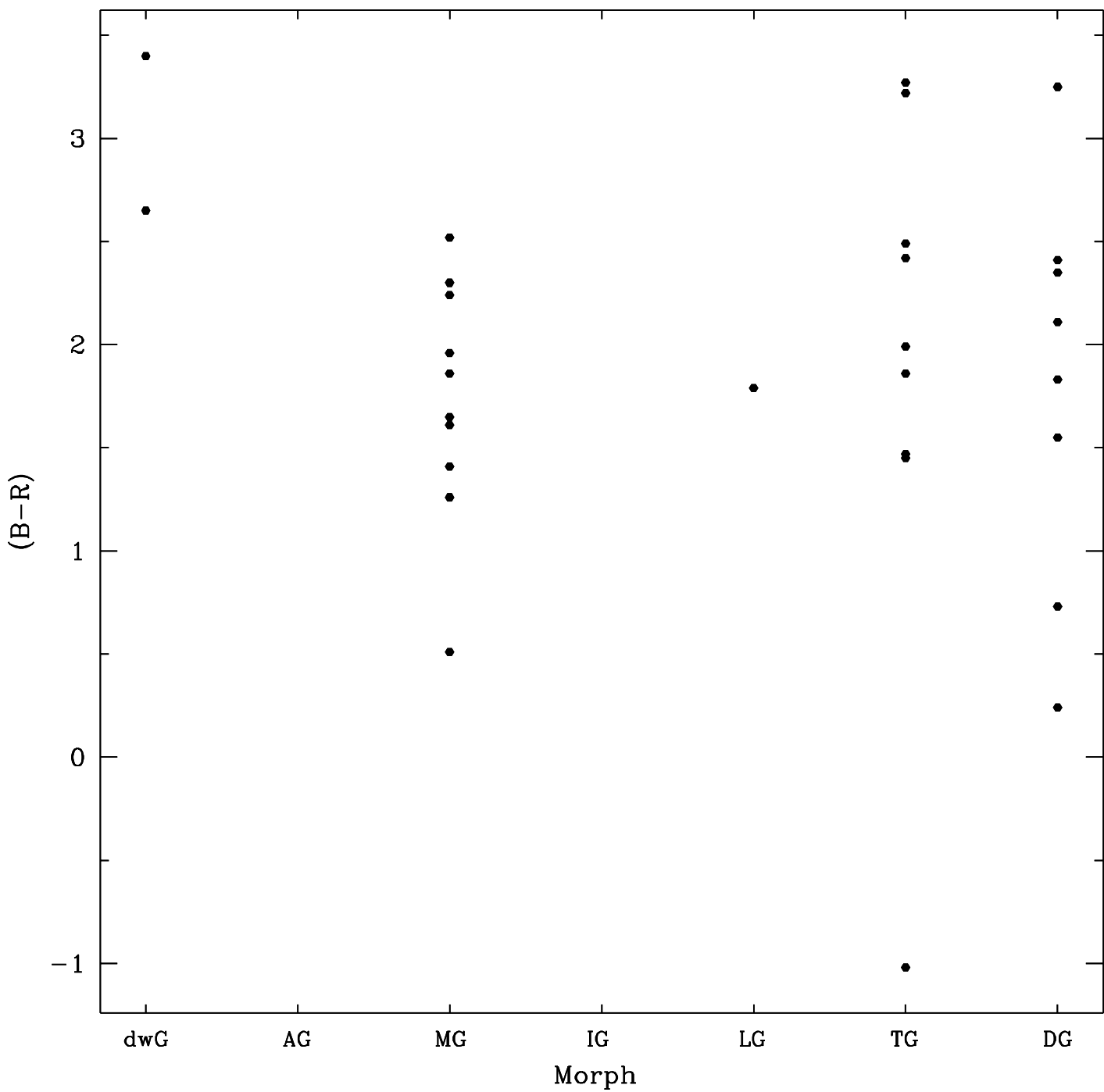


Figure 11

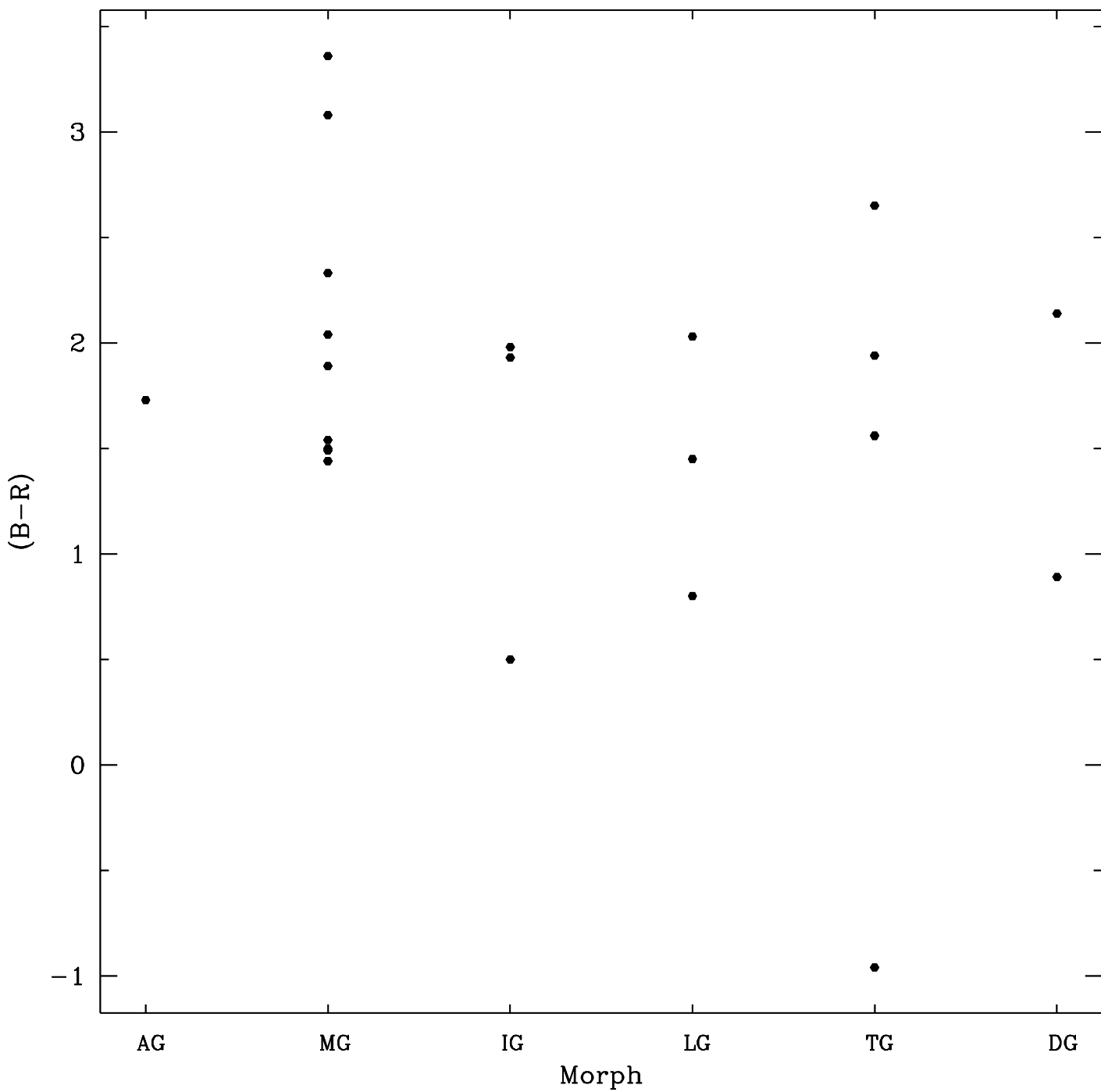


Figure 12

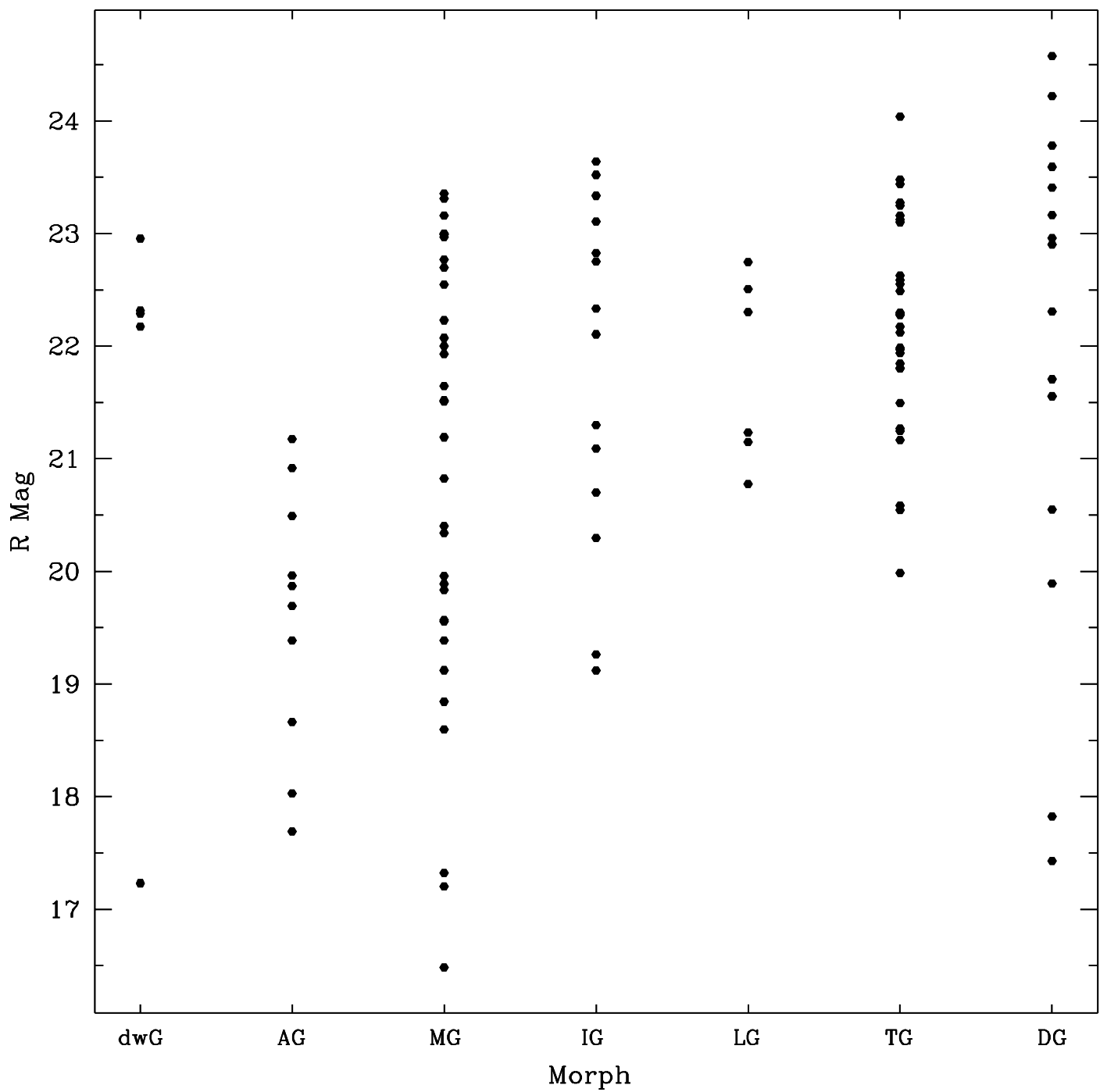


Figure 13

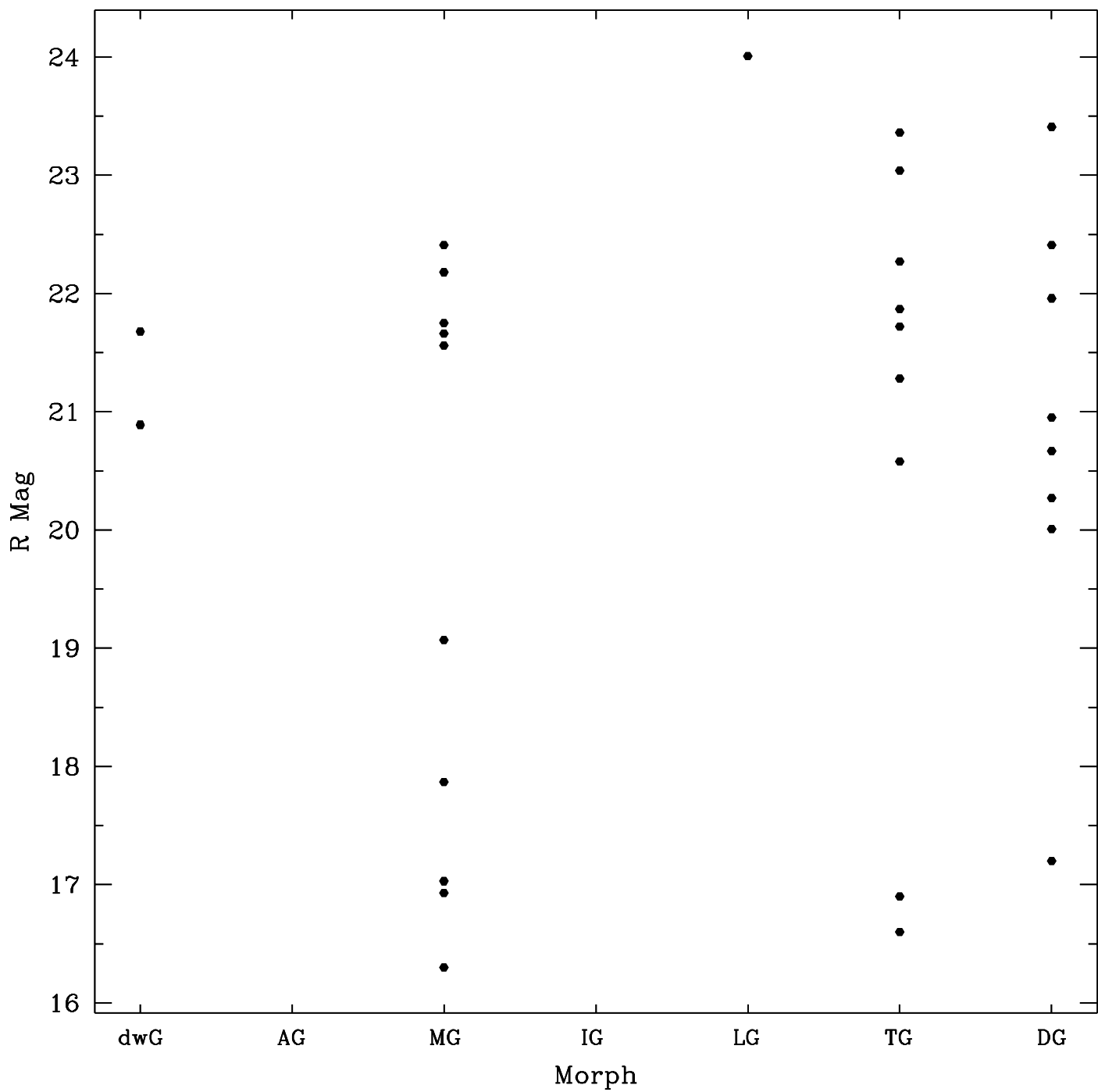


Figure 14

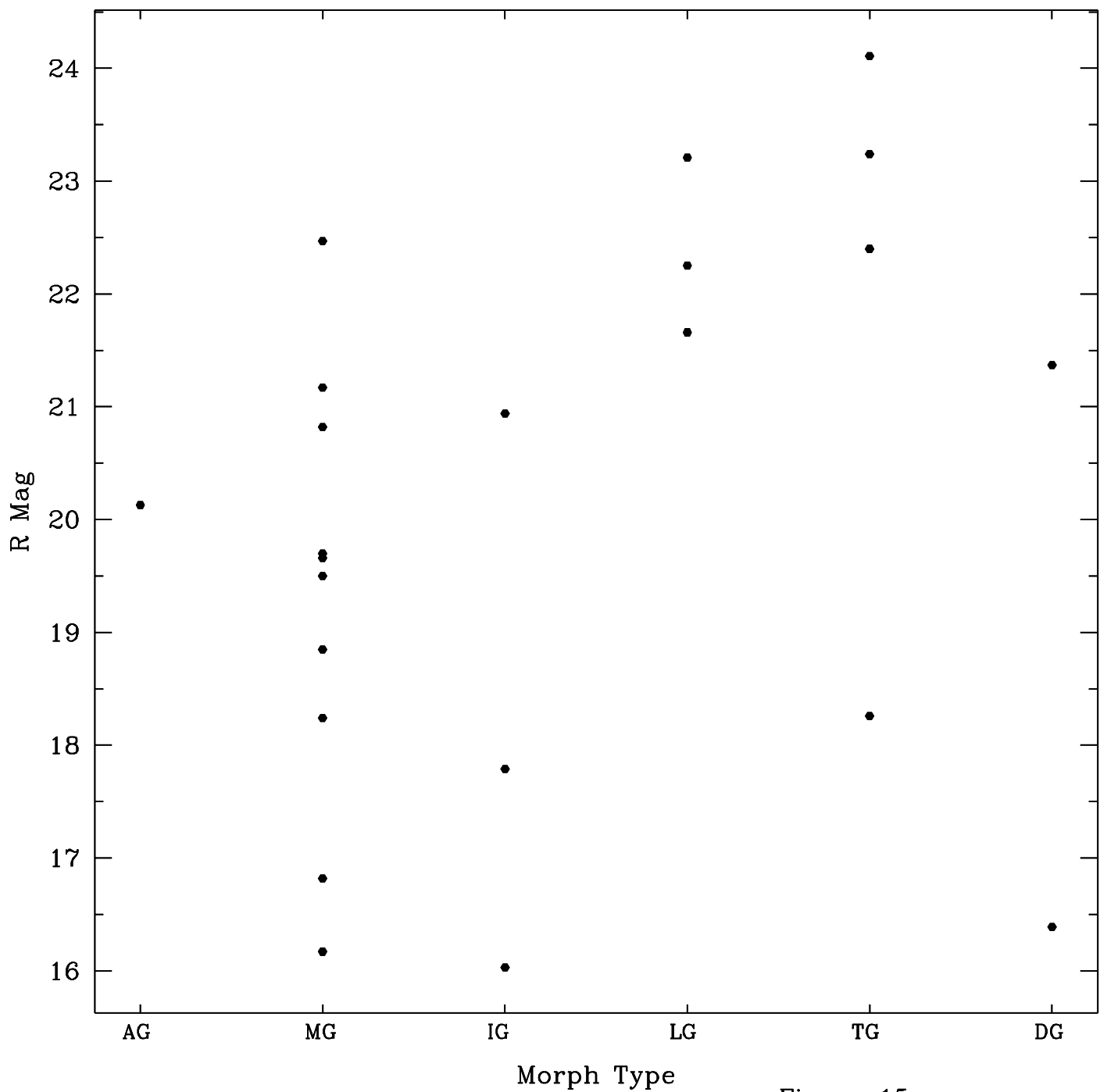


Figure 15

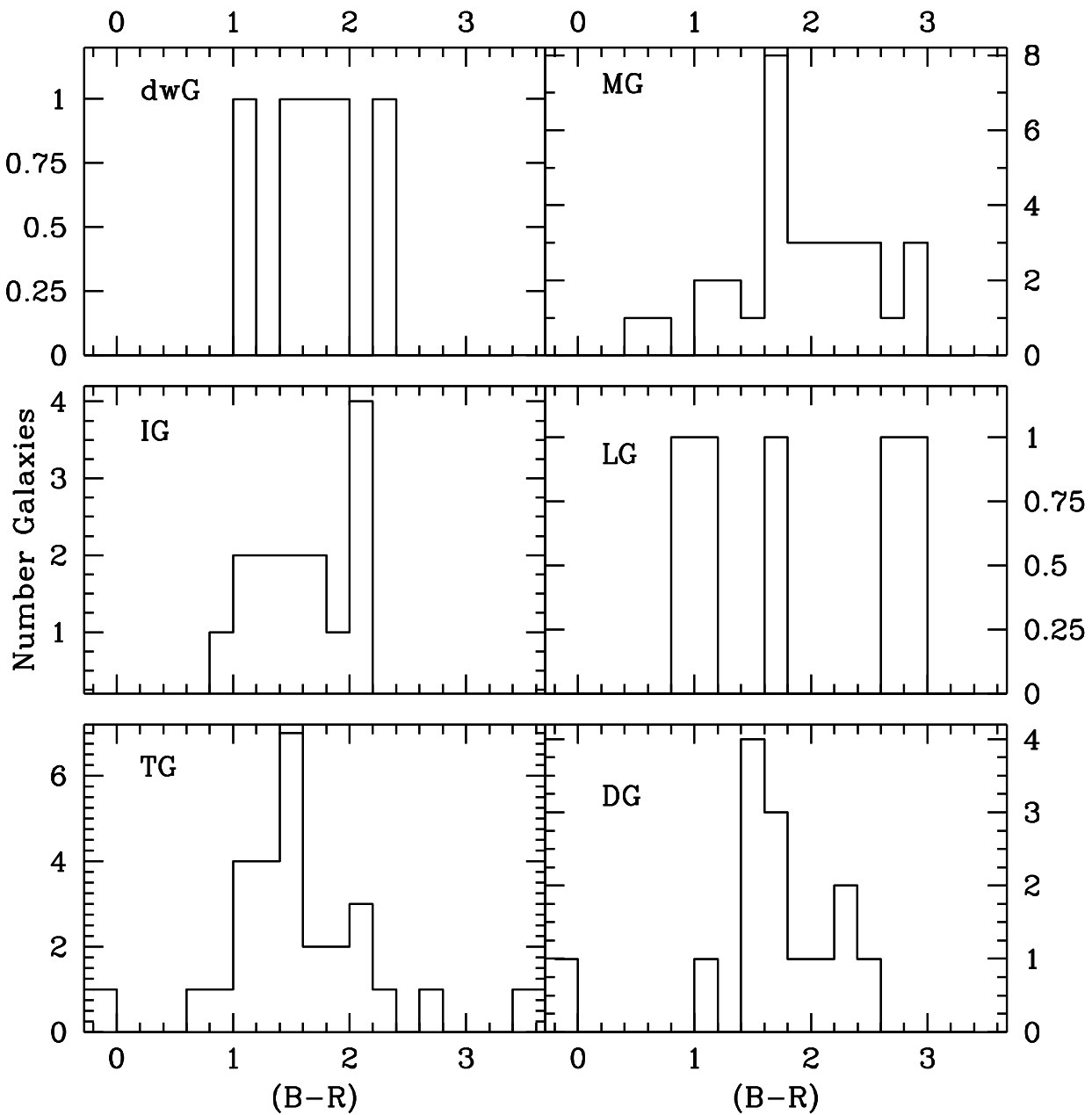


Figure 16

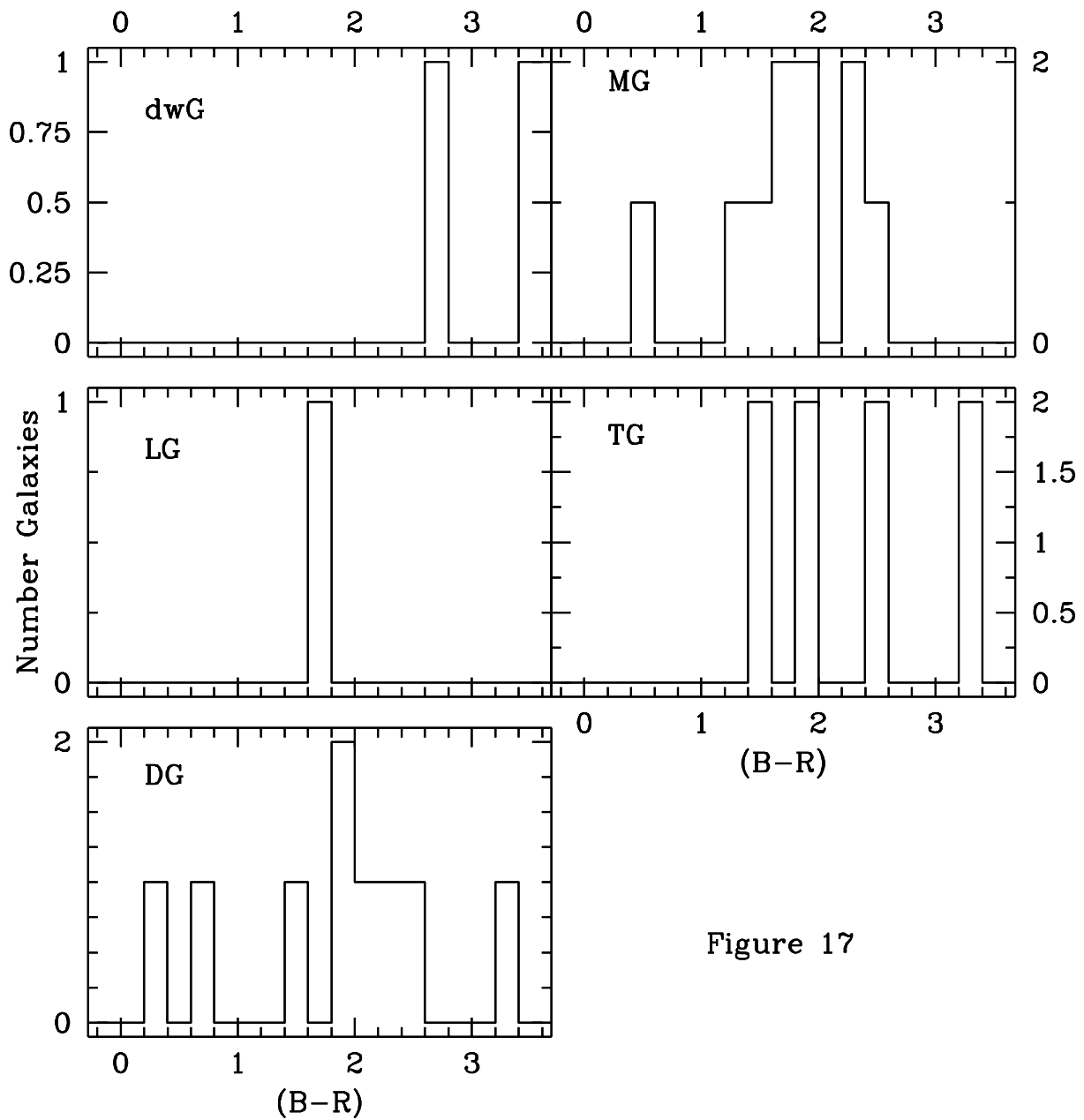


Figure 17

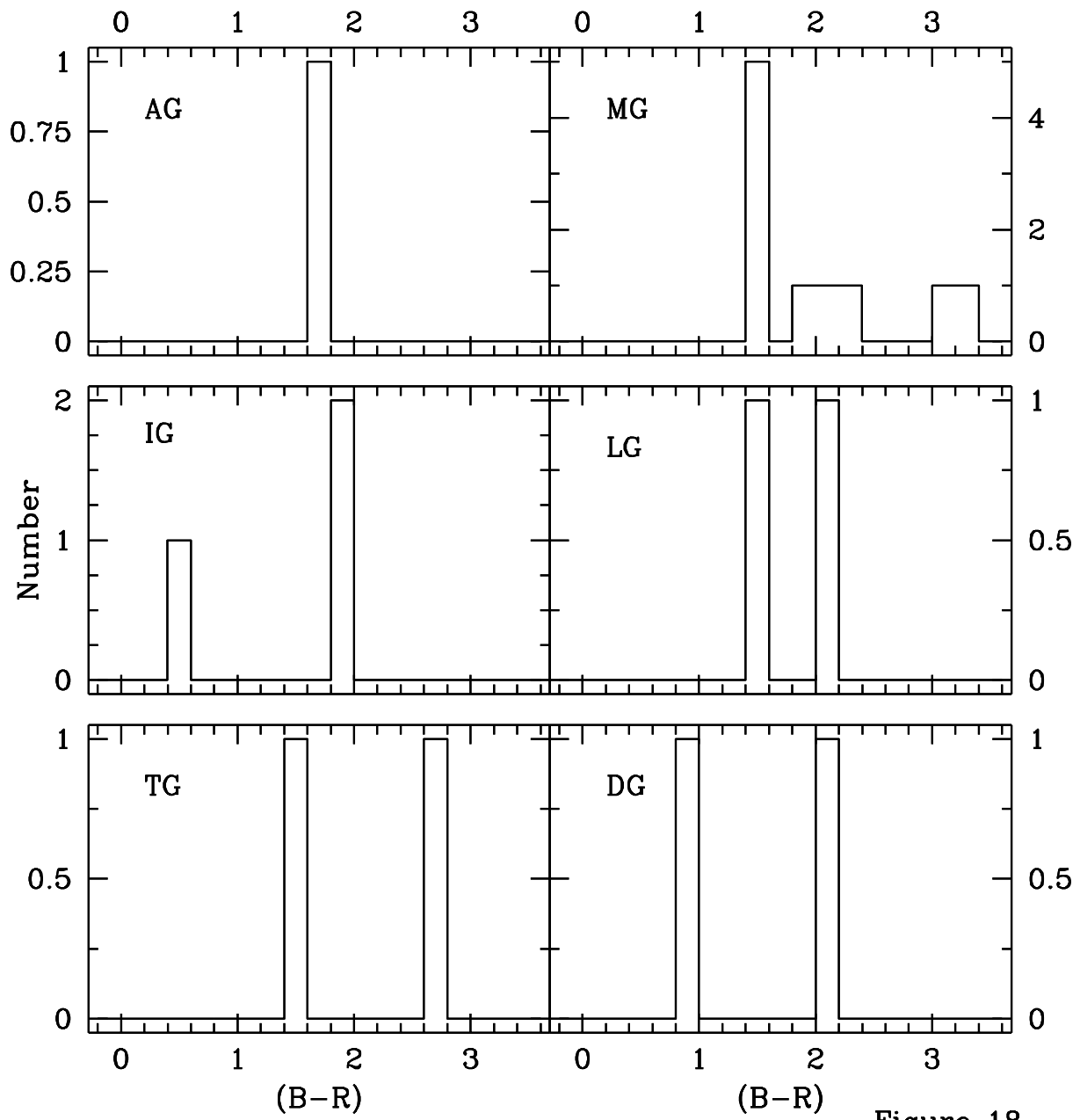


Figure 18

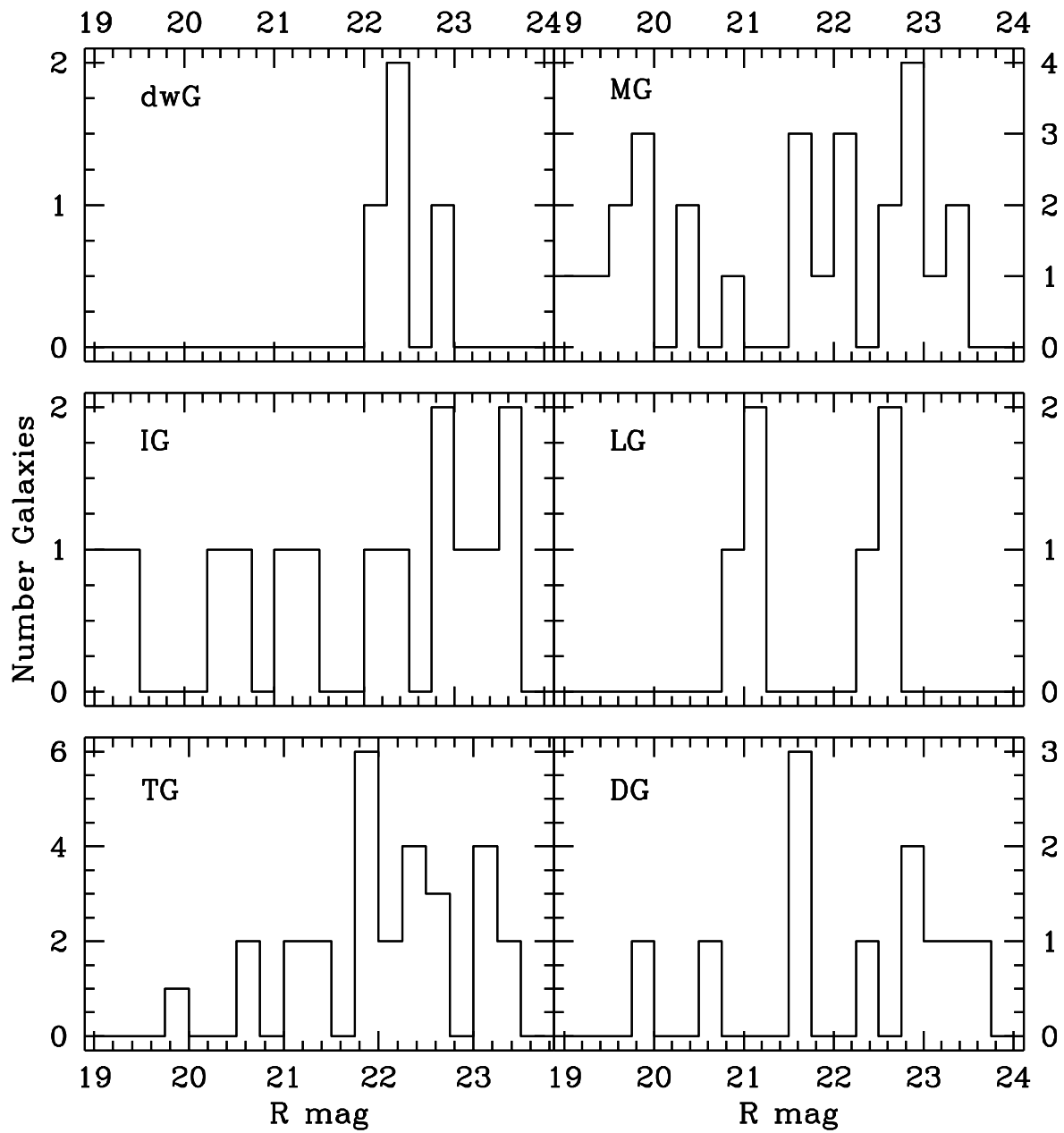


Figure 19

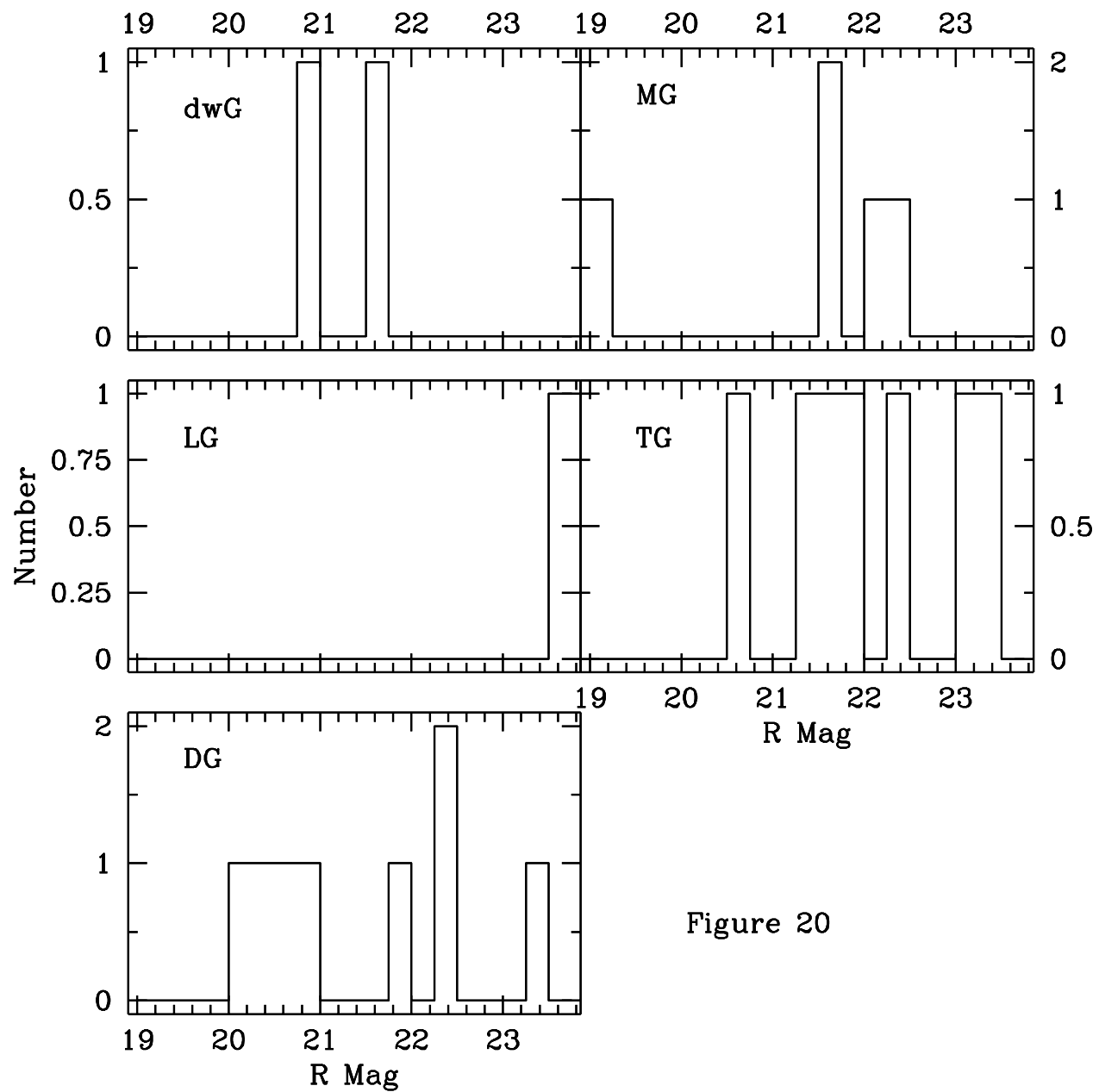


Figure 20

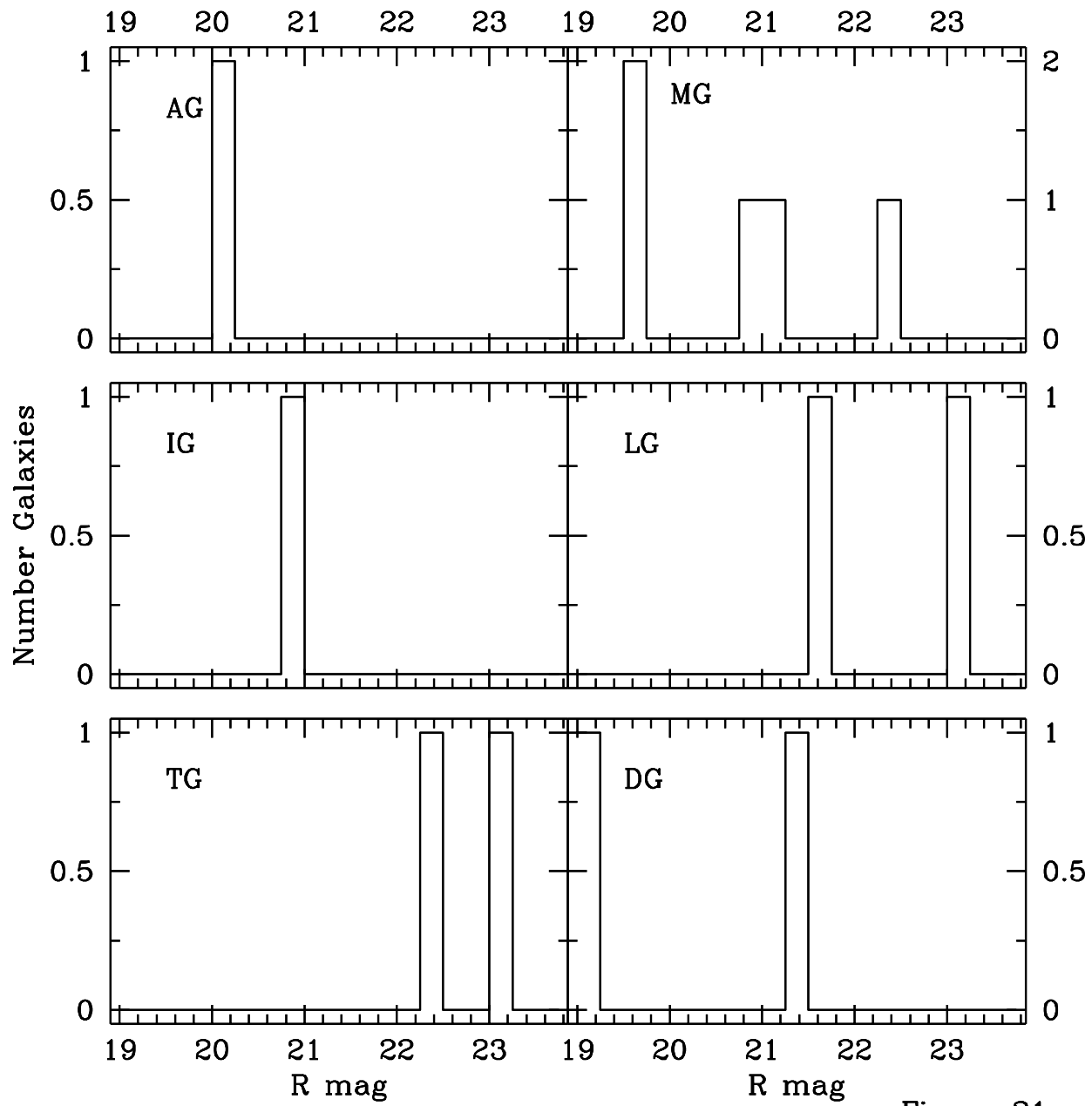


Figure 21